



**HAL**  
open science

# The adhesion of homogenized fat globules to proteins is increased by milk heat treatment and acidic pH: Quantitative insights provided by AFM force spectroscopy

Sameh Obeid, Fanny Guyomarc'H, Gaëlle Tanguy-Sai, Nadine Leconte, Florence Rousseau, Anne Dolivet, Arlette Leduc, Xiaoxi Yu, Chantal Cauty, Gwénaél Jan, et al.

## ► To cite this version:

Sameh Obeid, Fanny Guyomarc'H, Gaëlle Tanguy-Sai, Nadine Leconte, Florence Rousseau, et al.. The adhesion of homogenized fat globules to proteins is increased by milk heat treatment and acidic pH: Quantitative insights provided by AFM force spectroscopy. Food Research International, 2020, 129, pp.108847. 10.1016/j.foodres.2019.108847 . hal-02405809

**HAL Id: hal-02405809**

**<https://hal.science/hal-02405809>**

Submitted on 21 Jul 2022

**HAL** is a multi-disciplinary open access archive for the deposit and dissemination of scientific research documents, whether they are published or not. The documents may come from teaching and research institutions in France or abroad, or from public or private research centers.

L'archive ouverte pluridisciplinaire **HAL**, est destinée au dépôt et à la diffusion de documents scientifiques de niveau recherche, publiés ou non, émanant des établissements d'enseignement et de recherche français ou étrangers, des laboratoires publics ou privés.



Distributed under a Creative Commons Attribution - NonCommercial - NoDerivatives 4.0 International License

1  
2  
3  
4  
5  
6  
7  
8  
9  
10  
11  
12  
13  
14  
15  
16

**The adhesion of homogenized fat globules to proteins is increased by milk heat treatment and acidic pH: quantitative insights provided by AFM force spectroscopy**

Sameh Obeid<sup>1</sup>, Fanny Guyomarc'h<sup>1</sup>, Gaëlle Tanguy<sup>1</sup>, Nadine Leconte<sup>1</sup>, Florence Rousseau<sup>1</sup>, Anne Dolivet<sup>1</sup>, Arlette Leduc<sup>1</sup>, Xiaoxi Wu<sup>1</sup>, Chantal Cauty<sup>1</sup>, Gwénaél Jan<sup>1</sup>, Frédéric Gaucheron<sup>2</sup>, Christelle Lopez<sup>1,3,\*</sup>

<sup>1</sup> INRA, UMR1253 STLO, Agrocampus Ouest, 35000 Rennes, France

<sup>2</sup> CNIEL, 75009 Paris, France

<sup>3</sup> INRA, UR1268 BIA, 44300 Nantes, France

\*Corresponding author

E-mail address: [christelle.lopez@inra.fr](mailto:christelle.lopez@inra.fr)

17 **Abstract**

18 The rheological properties and microstructure of dairy gels involve the connectivity between  
19 milk fat globules (MFG) and casein micelles that is affected by technological processes such  
20 as milk homogenization and heat treatment. The underlying mechanisms require further  
21 quantification of the interactions at the nanoscale level to be fully understood and controlled.  
22 In this study, we examined the adhesion of homogenized MFG to milk proteins and evaluated  
23 the role of ultra-high temperature (UHT) heat treatment and pH. The combination of physico-  
24 chemical analysis, rheology and microscopy observations at different scale levels associated  
25 to atomic force microscopy (AFM) force spectroscopy were used. AFM experiments  
26 performed at the particle scale level showed that adhesion of individual homogenized MFG to  
27 milk proteins (1) is increased upon acidification at pH 4.5: 1.4 fold for unheated samples and  
28 3.5 fold for UHT samples, and (2) is enhanced by about 1.7 fold at pH 4.5 after UHT heat  
29 treatment of milk, from 176 pN to 296 pN, thanks to highly-reactive heat-denatured whey  
30 proteins located at the surface of MFG and caseins. The increased inter-particle adhesion  
31 forces accounted for more connected structures and stiffer UHT milk acid gels, compared to  
32 unheated-milk gels. Using a multiscale approach, this study showed that heat treatment of  
33 milk markedly affected the interactions occurring at the particle's surface level with  
34 consequences on the bulk structural and rheological properties of acid gels. Such findings will  
35 be useful for manufacturers to modulate the texture of fermented dairy products through the  
36 tailoring of heat-induced complexation of proteins and the connectivity of homogenized MFG  
37 with the protein network. This work will also contribute in a better understanding of the  
38 impact of process-induced changes on the digestibility and metabolic fate of proteins and  
39 lipids.

40

41 **Keywords:** Milk fat globule surface, Whey protein aggregate, Homogenization, Interface,  
42 Emulsion, Protein network, Acid dairy gel, Processed-induced changes, Atomic force  
43 microscopy

44

## 45        **1. Introduction**

46        The transformation of milk into dairy products involves many mechanical (e.g.  
47        homogenization), thermal (e.g. pasteurization, ultra-high temperature) and chemical (e.g.  
48        acidification) treatments. Such processes alter the structure of milk components, including  
49        milk fat globules (MFG) and casein micelles, as well as their surface properties and their  
50        connectivity through changes in the lipid–protein and protein–protein interactions. In  
51        consequence, the microstructure and rheological properties of dairy products are affected.  
52        However, the mechanisms underlying such structural and rheological changes remain poorly  
53        known at the particle scale level and require further investigations.

54        Milk is a natural oil-in-water emulsion composed of MFG (mean diameter 4  $\mu\text{m}$ ) dispersed in  
55        a suspension of proteins including the colloidal casein micelle assemblies (100 – 200 nm  
56        diameter; 80% w/w of milk proteins) and soluble whey proteins (WP; 20% w/w of milk  
57        proteins). The MFG consist of a core of triacylglycerol (TAG; 98% of the milk lipids)  
58        surrounded by a biological membrane, organized as a trilayer of polar lipids, cholesterol and  
59        glycoproteins, called the milk fat globule membrane (MFGM) (Lopez, 2011). The colloidal  
60        casein micelle assemblies are composed of  $\kappa$ -,  $\beta$ -,  $\alpha_{s1}$ - and  $\alpha_{s2}$ -caseins maintained by  
61        intermolecular hydrophobic interactions and calcium phosphate bridges. The glycosylated end  
62        of the peripheral  $\kappa$ -caseins forms an electronegative polymer brush that provides electrostatic  
63        and steric stability of the colloidal casein micelle assemblies at the milk pH, i.e. pH 6.7  
64        (Dalglish, 2011). Casein micelles are stable upon heating until 100°C (Dalglish, 2011;  
65        Gaucheron, 2005), but readily precipitate into gels upon acidification, through neutralization  
66        of their surface charge at about pH 4.6 and collapse of their  $\kappa$ -casein brush (Gaucheron, 2005;  
67        Tuinier & de Kruif, 2002). WP are globular proteins whose native form is soluble across a  
68        wide range of pH. They consist of  $\beta$ -Lactoglobulin ( $\beta$ -Lg; 51% w/w of WP),  $\alpha$ -Lactalbumin  
69        ( $\alpha$ -La; 22% w/w of WP) and other minor proteins (Farrell et al., 2004). In contrast to casein  
70        micelles, WP are heat-sensitive. Heat-treatment above 70°C induces denaturation of the WP,  
71        leading to exposure of reactive-thiol groups and to WP aggregation through intermolecular  
72        hydrophobic interactions and formation of intermolecular disulfide bridges. In milk, the thiol-  
73        containing  $\kappa$ -caseins, and to a minor extent  $\alpha_{s2}$ -caseins, can co-aggregate with the denatured  
74        WP, mainly  $\beta$ -Lg, inducing the attachment of a significant fraction of the WP aggregates onto  
75        the surface of casein micelles (Anema & Li, 2003b; Donato & Guyomarc'h, 2009; Vasbinder  
76        & de Kruif, 2003). The denatured WP do not stay soluble upon acidification and bear  
77        significant hydrophobicity. Authors showed that the presence of heat-induced WP aggregates

78 increases the firmness of acid skimmed milk gels (Morand, Dekkari, Guyomarc'h, &  
79 Famelart, 2012; Vasbinder & de Kruif, 2003). Therefore, heat treatment of milk can be used  
80 to modulate protein – protein interactions, and thus the texture of dairy products. However,  
81 scientific knowledge about the impact of heat-induced WP on the connectivity between  
82 homogenized MFG and the protein network in acid gels needs to be improved.

83 Heat treatment of milk (pasteurization, sterilization by ultra-high-temperature (UHT)) is  
84 performed in the dairy industry to ensure its microbiological safety and increase its shelf-life  
85 by decreasing the amount of bacteria, but also to modulate the texture of dairy products by  
86 inducing the denaturation of WP. Homogenization of milk is a mechanical process used to  
87 improve the physical stability of the emulsion by decreasing the size of MFG. The high shear  
88 stress applied during homogenization breaks up the 4- $\mu\text{m}$  diameter MFG into MFG with  
89 diameters below 1  $\mu\text{m}$  (Lopez, Cauty & Guyomarc'h, 2015). Furthermore, homogenization  
90 leads to the disruption of the MFGM and induces the adsorption of milk proteins, i.e. casein  
91 micelles and some native WP (below 5-7% of total adsorbed proteins), onto the newly formed  
92 surface of MFG (Lee & Sherbon, 2002; Ye, Anema, & Singh, 2008). In the dairy industry,  
93 homogenization of milk is combined with heat treatments. As an example, commercially  
94 available milk is commonly homogenized and heat-treated using pasteurization or UHT  
95 processing. In milks previously heated at temperatures above 70°C, the homogenization leads  
96 to adsorption of denatured WP onto the MFG surface that can reach 10-25% of the adsorbed  
97 proteins (García-Risco, Ramos, & López-Fandiño, 2002; Lee & Sherbon, 2002; Ye, Anema &  
98 Singh, 2008). Therefore, the introduction of a heating step prior to homogenization modifies  
99 the surface composition of homogenized MFG. Acidification of milk is a widely used  
100 chemical treatment that is involved in the production of dairy products, e.g. sour creams and  
101 yoghurts. Acidification is also a natural chemical mechanism occurring upon food digestion in  
102 the stomach that leads to the formation of a coagulum upon milk gastric digestion. The  
103 decrease in pH leads to the physical instability of the casein micelles alone or in interaction  
104 with the heat-sensitive WP, and to the formation of a protein network in which MFG can be  
105 more or less strongly entrapped depending on their surface properties. Upon gelation,  
106 homogenized MFG interact with the protein matrix, thereby increasing the gel's elastic  
107 modulus (Lopez & Dufour, 2001; Michalski, Cariou, Michel, & Garnier, 2002; van Vliet,  
108 1988). Process-induced changes in the microstructure and rheological properties of milk at  
109 acid pH, such as those occurring after homogenization and heat-treatment, can have  
110 consequences on the mechanisms involved in MFG and protein digestion (Garcia, Antona,

111 Robert, Lopez & Armand, 2014; Liang, Qi, Wang, Jin, & McClements, 2017; Mulet-Cabero,  
112 Mackie, Wilde, Fenelon, & Brodkorb, 2019; Ye, Cui, Dalglish, & Singh, 2017; Zhao, Du &  
113 Mao, 2019).

114 The impact of the main technological treatments involved in the dairy industry, i.e. heat-  
115 treatment, homogenization and acidification, on milk proteins and MFG has been widely  
116 investigated at the micro and macroscale (Michalski, Cariou, Michel, & Garnier, 2002; Lee  
117 and Sherbon, 2002; Jukkola and Rojas, 2017). However, information is lacking at the  
118 nanoscale on the role of the heat-denatured WP in modifying individual interaction between  
119 homogenized MFG and casein micelles in heated milk and acid gels. The main reason is the  
120 lack of experimental techniques allowing measurements directly from complex colloidal food  
121 systems at the relevant nanoscale level. Atomic force microscopy (AFM) is a well-adapted  
122 technique to image, with nanometer resolution, the surface topography of particles and to  
123 probe interaction forces with high sensitivity in the pN to nN range (Müller, Krieg, Alsteens,  
124 & Dufrêne, 2009). In recent years, AFM has gained growing interest in studying complex  
125 food systems (Gunning & Morris, 2018; West & Rousseau, 2018). In a previous study, we  
126 successfully used AFM force spectroscopy to investigate the impact of homogenization and  
127 pH on the adhesion forces between individual MFG and AFM probes functionalized with  
128 casein micelles (Obeid, Guyomarc'h, Francius, Guillemin, Wu, Pezennec, Famelart, Cauty,  
129 Gaucheron & Lopez, 2019). AFM experiments showed that casein-coated homogenized MFG  
130 interacted with higher adhesion forces to surrounding casein micelles, compared to native  
131 MFG covered by the MFGM with dense repulsive glycocalyx. The adhesion forces were  
132 increased at pH 4.5, with 109 pN for native MFG vs. 210 pN for homogenized MFG. This  
133 first study on MFG showed that AFM force spectroscopy is a promising technique to quantify  
134 adhesion forces at the particle scale level in complex systems such as food emulsions.

135 The present study was designed to determine whether the denaturation of WP and their  
136 interactions with casein micelles, induced by UHT heat treatment, could modulate the  
137 connectivity between homogenized MFG and the protein network formed at acidic pH. We  
138 examined the composition and surface properties of MFG and casein micelles, and quantified  
139 by AFM force spectroscopy the adhesion forces between individual homogenized-MFG and  
140 bulk proteins (i.e. casein micelles and WP). By using a multiscale approach, we related the  
141 adhesion forces measured at the individual particle level with the bulk characteristics of the  
142 milk acid gels, i.e. their microstructure and rheological properties.

143

## 144 2. Materials and methods

### 145 2.1. Materials

146 Bulk tank raw whole bovine milk was provided by Gaec des Fougères (La Chapelle des  
147 Fougeretz, France). Glucono-delta-lactone (GDL), Fast-Green FCF and Nile-Red fluorescent  
148 dyes were purchased from Sigma-Aldrich (St Louis, USA). D(+)-sucrose was purchased from  
149 VWR Chemicals (St Louis, USA). PIPES buffer was used as previously reported in [Obeid et](#)  
150 [al. \(2019\)](#). PIPES buffer (1,4-piperazinediethane sulfonic acid) contained 10 mM PIPES, 50  
151 mM NaCl, and 2 mM CaCl<sub>2</sub>, all purchased from Sigma-Aldrich. The PIPES buffer was  
152 adjusted to pH 6.7 or 4.5, using 1M NaOH or HCl respectively.

153

### 154 2.2. Preparation of milk samples and isolation of casein micelles

155 Homogenized (H-) and UHT-homogenized (UHT-H-) milks, as well as native- and UHT-  
156 skimmed milks were prepared from the same raw milk, using the technological facilities of  
157 the INRA STLO dairy platform (Rennes, France). The pH of native milk, originally of 6.6 at  
158 30°C, was adjusted to 6.5 in order to promote the interaction between denatured-WP and  
159 casein micelles upon heat treatment ([Anema & Li, 2003b](#); [Vasbinder & de Kruif, 2003](#)). To  
160 prepare H-milk, the milk was heated to 50°C for 10 min and homogenized at 20 MPa (2 MPa  
161 in the 2<sup>nd</sup> stage) with a high-pressure homogenizer Panda Plus 2000 (GEA Niro Soavi, Parma,  
162 Italy; Flow: 9 L/h). To prepare UHT-H-milk, the milk was preheated from 40°C to 90°C (3  
163 °C/sec) and from 90°C to 140°C (3 °C/sec) and immediately UHT heat treated at 140°C for 4  
164 sec using an indirect UHT processing system (Microthermics UHT/HTST Lab 25 EDH,  
165 Microthermics Inc., Raleigh, NC, USA). The UHT-milk was then rapidly cooled at 9 °C/sec  
166 prior to homogenization at 20 MPa (2 MPa in the 2<sup>nd</sup> stage) with the high-pressure  
167 homogenizer Panda Plus 2000. Sodium-azide (0.02% w/v) was added to the milk samples in  
168 order to prevent bacterial growth. Milk samples were stored at 20 ± 1 °C and used within the  
169 next three days after milk processing.

170 In order to isolate native- and UHT-casein micelles for AFM force spectroscopy experiments  
171 (i.e. grafting of the AFM probes), the skimmed counterparts of the native and UHT-milks  
172 were prepared. Raw milk at pH 6.5 was skimmed at 50°C using an Elecrem separator  
173 (Vanves, France), then subjected to the same UHT heat treatment as described above for  
174 whole milk. Native- and UHT-casein micelles were isolated from native- and UHT-skimmed  
175 milks respectively to eliminate residual WP and other solutes. Briefly, skimmed milks were

176 diafiltered 5-fold using PIPES buffer pH 6.7 using a lab-scale Centramate tangential filtration  
177 system with 0.1  $\mu\text{m}$ -cut-off membranes (Centramate cassettes, Pall Corporation, Saint  
178 Germain-en-Laye, France). Isolated casein micelles in PIPES buffer pH 6.7, with a final  
179 concentration of about 20  $\text{g}\cdot\text{kg}^{-1}$ , were aliquoted and stored at  $-20^{\circ}\text{C}$  until use for AFM force  
180 spectroscopy experiments.

181

### 182 **2.3. Denaturation rate of the whey proteins**

183 The total nitrogen (TN), non-casein nitrogen (NCN) and non-protein nitrogen (NPN) contents  
184 were determined by the Kjeldahl method (IDF Standard 20B, 1993; ISO 8968-1, 2014; ISO  
185 8968-4, 2016; ISO 17997-1, 2004), for native milks, H-milks, UHT-H-milks and skimmed  
186 milks, prior to or after UHT heat treatment. Nitrogen content was converted into equivalent  
187 protein content using 6.38, 6.25 and 6.19 as conversion factors for TN, NCN and NPN,  
188 respectively (Karman & Van Boekel, 1986). The amount of native WP was calculated as  
189 [Native WP] = [NCN] - [NPN]. Proteins that precipitate at pH 4.6, i.e. essentially caseins but  
190 also the denatured WP in heated samples, were calculated as [CN] = [TN] - [NCN]. From  
191 this, the respective amounts of denatured WP and caseins in [CN] of the heated samples, as  
192 well as the rate of WP denaturation, were calculated knowing [Native WP] and [CN] of the  
193 unheated milk reference.

194

### 195 **2.4. Washing of homogenized milk fat globules**

196 For the determination of the interfacial protein composition by gel electrophoresis and for  
197 AFM experiments, MFG were isolated from the milk aqueous phase to remove un-adsorbed  
198 proteins according to a method adapted from Patton & Huston (1986). Briefly, H- or UHT-H  
199 milks were warmed to  $50^{\circ}\text{C}$ , then 10 g of milk was mixed with 5 g of PIPES buffer pH 6.7  
200 containing 50% w/w of sucrose. Then, in 50 mL plastic centrifuge tubes, 15 g of the treated  
201 milk were delivered under 30 g of a solution of PIPES buffer pH 6.7 containing 5% w/w of  
202 sucrose. The tubes were centrifuged at 2500 g for 30 min in order to form a layer of washed  
203 homogenized MFG at the top of the tubes. The protocol used for native MFG has been  
204 previously described (Obeid, Guyomarc'h, Francius, Guillemin, Wu, Pezennec, Famelart,  
205 Cauty, Gaucheron & Lopez, 2019).

206

### 207 **2.5. Gel electrophoresis**



208 After washing of MFG, the centrifuge tubes were frozen then cleaved just below the washed  
209 MFG layer. Collected MFG were diluted twice in SDS 1% w/w and centrifuged at 2500 g for  
210 30 min to recover the desorbed interfacial proteins in the lower phase. Interfacial proteins  
211 desorbed from native-, H- and UHT-H-MFG as well as the proteins in isolated native- and  
212 UHT-casein micelle samples were quantified by micro-Kjeldahl method and analyzed by  
213 SDS-PAGE. The different protein samples were diluted in denaturing and reducing buffer  
214 containing 0.5 M Tris-HCl pH 6.8, 20% glycerol, 2% SDS, containing 0.5% bromophenol  
215 blue and 40 mM dithiothreitol (a reducing agent that breaks down the disulfide linkages  
216 responsible of the aggregation of heat-denatured WP) for 1 h at 37°C. As an alternative, in  
217 non-reducing conditions, protein samples were diluted in a similar buffer, but without  
218 dithiothreitol, to keep the disulfide bonds. Each diluted protein sample was then loaded on a  
219 sample well (10 µg of protein/well) on top of a precast 4-20% polyacrylamide gel  
220 electrophoresis (mini-protein TGX precast gel, Bio-Rad Laboratories, Dublin, Ireland).  
221 Electrophoresis was carried out at a constant current of 200 V for 45 min. Gels were rinsed  
222 with distilled water and were stained with Bio-safe Coomassie G250 stain (Bio-Rad  
223 Laboratories, Dublin, Ireland). A molecular weight (MW) marker (kit Precision Plus Protein  
224 Standards 10-250 kD, Bio-Rad Laboratories, Dublin, Ireland) was employed for MW  
225 calibration. The gels were scanned by an Image Scan II gel imager using the LabScan  
226 software (GE Healthcare, Velizy Villacoublay, France).

227

## 228 **2.6. Size and zeta-potential measurements**

229 The size distribution of MFG and the hydrodynamic diameter ( $D_h$ ) of casein micelles were  
230 determined by laser light scattering (Mastersizer 2000, Malvern Instruments, Orsay, France)  
231 and by dynamic light scattering (NanoSizer-ZS, Malvern Instruments, Orsay, France),  
232 respectively, as detailed in [Obeid et al. \(2019\)](#). Briefly, for MFG size distribution  
233 measurements, samples were diluted in ultra-pure water in the absence or presence of 1%  
234 SDS to check for possible flocculation of processed MFG. To determine the  $D_h$  of casein  
235 micelles, samples were diluted 100 fold v/v in PIPES buffer at pH 6.7. Measurements were  
236 carried out at 20°C.

237 The electrophoretic mobility of MFG and casein micelles was measured at 20°C using a  
238 Zetasizer Nano ZS (Malvern Instruments, Orsay, France), after dilution of the samples to  
239 1/1000 v/v in PIPES buffer at pH 6.7 or 4.5. The apparent  $\zeta$ -potential was deduced using the  
240 Henry's equation and the Smoluchowski approximation.

241 All measurements, size and  $\zeta$  –potential, were performed in triplicate and expressed as mean  
242 with standard deviation. Analyses of variance (ANOVA) were performed using the General  
243 Linear Model procedure of Statgraphics Plus version 5 (Statistical Graphics Corp.,  
244 Englewood Cliffs, NJ). Differences between the sample means were compared at the 5% level  
245 of significance using Fisher's least significance difference test.

246

## 247 **2.7. Rheological measurements**

248 The visco-elastic properties of H-milks and UHT-H-milks were measured as a function of pH  
249 as previously described in [Obeid et al. \(2019\)](#). Rheological measurements were carried out at  
250 50°C by small amplitude oscillatory rheology using a DHR-2 instrument (TA Instruments,  
251 Guyancourt, France) with coaxial cylinders. The storage modulus,  $G'$  (in Pa), was monitored  
252 as function of the pH, upon addition of 1.65% w/w GDL in milk samples, at a frequency of 1  
253 Hz and 1% strain. The gelation pH was established as the intercept of a linear extrapolation of  
254 the rapidly rising storage modulus  $G'$  with the pH axis. The final  $G'$  value was taken at pH  
255 4.5. Measurements were performed in triplicate and expressed as mean with standard  
256 deviation. ANOVA was performed using the General Linear Model procedure of Statgraphics  
257 Plus version 5. Differences between the sample means were compared at the 5% level of  
258 significance using Fisher's least significance difference test.

259

## 260 **2.8. Microscopy experiments**

### 261 **2.8.1. Transmission electron microscopy**

262 Transmission electron microscopy (TEM) was used to examine the homogenized milk and the  
263 UHT-homogenized milk. Briefly, H-milk and UHT-H-milk samples were solidified in agar  
264 1.5% (w/v), cut into 1 mm pieces, fixed overnight with 25 g.kg<sup>-1</sup> glutaraldehyde in 0.1 M Na-  
265 cacodylate and post-fixed for 1h in 1% osmium tetroxide. The pieces were then dehydrated  
266 through increasing ethanol concentrations, infiltrated and embedded in Epon resin mixture  
267 (Electron Microscopy Sciences), then finally polymerized at 60°C for 24 h. Ultra-thin sections  
268 were cut using a Leica ultra-microtome and stained with 4% uranyl-acetate for 1h. Sections  
269 were observed with JEOL-1400 TEM microscope operating at 120 kV. TEM images were  
270 recorded on camera Gatan Orius SC-1000.

271

### 272 **2.8.2. Confocal laser scanning microscopy**

273 Confocal laser scanning microscopy (CLSM) experiments were performed with an inverted  
274 Eclipse-TE2000-C1si confocal microscope (NIKON, Champigny sur Marne, France) to  
275 investigate the microstructure of milks and acid gels, as described in Obeid et al. (2019). A  
276 He-Ne laser operating at 543 nm wavelength excitation, a laser diode operating at 642 nm  
277 and a x100 (NA 1.4) oil immersion objective were used. The TAG core of MFG was stained  
278 with Nile-Red fluorescent dye (exc. 543 nm). The proteins were stained using Fast-Green  
279 FCF (exc. 642 nm). After labeling, the samples were kept at 20°C for 30 min prior to CLSM  
280 observations. For observations at acid pH, the fluorescently-labeled milk samples were  
281 acidified by adding GDL (1.65 % w/w), incubated at 50°C and then observed when the milk  
282 gel reached pH 4.5.

283 An inverted CLSM Zeiss LSM 880 microscope (Carl Zeiss SAS, Marly Le Roi, France) was  
284 used to observe the modified AFM probes, using a laser at 561 nm (spectral detection range:  
285 560 - 601 nm). AFM probes were incubated overnight at 4°C with fluorescent  $\alpha_{s1}$ -caseins  
286 conjugated to Rhodamine-B-IsoThioCyanate (RITC) at 10 mg/mL in PIPES buffer pH 6.7 in  
287 PIPES buffer. The observations were performed using a x63 oil immersion objective.

288

### 289 **2.8.3. Atomic force microscopy imaging and force spectroscopy**

290 AFM experiments, imaging and force spectroscopy, were carried out at  $22 \pm 1^\circ\text{C}$  using an  
291 MFP-3D Bio AFM (Asylum Research, Oxford Instruments, Santa Barbara, CA, USA).

292 Washed H-MFG or UHT-H-MFG, suspended to 1:10 in PIPES buffer pH 6.7, were  
293 immobilized on Isopore polycarbonate track-etched Millipore filters of 0.6  $\mu\text{m}$  pore size by  
294 gently passing the solution through the filter membrane using a syringe, until blockage (**Fig.**  
295 **1-A**). The filter membrane was gently rinsed with buffer, in order to remove loosely  
296 immobilized MFG. The filter membrane was then attached inside a Petri dish using a double-  
297 sided adhesive tape, and immersed in PIPES buffer pH 6.7.

298 Imaging of immobilized MFG was performed in PIPES buffer, using silicon MSNL probes  
299 (Bruker Nano Surfaces, Santa Barbara, CA - nominal spring constant of  $0.01 \text{ N.m}^{-1}$ ) through  
300 the force-mapping mode, with a scan rate of 1Hz on  $10 \times 10 \mu\text{m}^2$  surface and at least  $64 \times 64$   
301 pixels. The adhesion force measurements were performed through the force-mapping mode  
302 by using casein micelles-modified AFM probes prepared as follows. AFM probes with  
303 attached 5- $\mu\text{m}$  borosilicate glass particles, coated with gold and modified with  $\text{NH}_3$  groups  
304 (Novascan, Ames, Iowa, USA; nominal spring constant of  $0.01 \text{ N.m}^{-1}$ ) were used. The AFM

305 probes were incubated overnight at 4°C in the dispersions of isolated native or UHT-casein  
306 micelles (20 g.kg<sup>-1</sup> ; thawed aliquots were left to equilibrated at 20°C for at least 1h before  
307 experiments prior to use to ensure complete rehydration and ionic balance of the casein  
308 micelles). The AFM probes were then washed and kept in PIPES buffer pH 6.7 until use. The  
309 successful grafting of caseins on the AFM probes was validated by CLSM experiments using  
310 fluorescent caseins (**Fig. 1-B**).

311 **Fig. 1-A** illustrates the two experimental set-ups that have been adopted to measure the  
312 adhesion forces between individual homogenized MFG and casein micelles, without or with a  
313 UHT heat treatment of the milks. On one hand, AFM measurements were performed between  
314 H-MFG and native casein micelles grafted on AFM probes (**Fig. 1-A-left**). On the other hand,  
315 measurements were performed between UHT-H-MFG and UHT-casein micelles grafted on  
316 AFM probes (**Fig. 1-A-right**). For each sample, adhesion force measurements were first  
317 performed in PIPES buffer at pH 6.7. Then, the PIPES buffer at pH 6.7 was replaced by  
318 PIPES buffer at pH 4.5 and the set-up was incubated for 30 min at this pH before starting  
319 again the force measurements. The force maps were recorded on 50 x 50 μm<sup>2</sup> surface and 30  
320 x 30 pixels with an applied force of 500 pN, a probe velocity of 1 μm.s<sup>-1</sup> and a contact time of  
321 1 sec. The cantilever spring constant was determined prior to each AFM force spectroscopy  
322 experiment using the thermal noise calibration method (Lévy & Maaloum, 2001). At least 3  
323 independent experiments were performed to measure the adhesion forces in each experimental  
324 set-up at pH 6.7 then pH 4.5.

325 Interactions between casein micelles-modified AFM probes and MFG produce specific  
326 adhesion peaks in the retraction force curves as reported in Obeid et al. (2019) and illustrated  
327 in **Fig. 1-C**. In each experimental condition, force curves showing non-specific adhesive  
328 events or deformed baseline were discarded (Le et al., 2013). Force curves with adhesion  
329 forces below 45 pN were considered as noise. Force curves evidencing specific adhesion were  
330 analyzed in order to determine the maximal adhesion force ( $F_{adh}$ ) and rupture distance ( $D_{adh}$ )  
331 as illustrated in **Fig. 1-C**. The AFM experimental data were statistically analysed using the  
332 Wilcoxon rank-sum test adapted for non-normally distributed data. Indeed, the distributions of  
333  $F_{adh}$  or  $D_{adh}$  were not Gaussian, because the measured adhesion involves objects (casein  
334 micelles, homogenized MFG) whose dimensions are not themselves normally distributed.  
335 Differences were considered statistically significant when P value < 0.001.

336

### 337 **3. Results and discussion**

### 3.1. UHT heat treatment leads to the denaturation of whey proteins in milk

338  
339 Compositions of the protein fractions (i.e. caseins, native- and denatured-WP) in the different  
340 milk samples are presented in **Fig. 2-A**. Casein fraction represented about 80% w/w of the  
341 total protein content in the different samples, in agreement with the literature (Dalglish,  
342 2011; Farrell et al., 2004). The percentage of native-WP was about 20% w/w in native milks  
343 and skimmed milks, in agreement with the literature (Ahmad et al., 2008; Farrell et al., 2004).  
344 Denatured-WP were not present in milk samples that were not subjected to UHT heat  
345 treatment (i.e. native milk, H-milk and skimmed milk samples). In contrast, about 16% w/w  
346 of total milk proteins corresponded to denatured-WP in milk samples that were subjected to  
347 UHT heat treatment, i.e. UHT-skimmed milk and UHT-H-milk (**Fig. 2-A**). This corresponds  
348 to about 80% w/w of the total WP in each sample. These results showed that, as expected,  
349 UHT heat treatment of milk induced significant denaturation of the WP (Anema & McKenna,  
350 1996; Oldfield, Singh, Taylor, & Pearce, 1998).

351

### 3.2. Surface properties of MFG and casein micelles in homogenized and UHT-homogenized milks

#### 3.2.1. UHT heat treatment alters the surface protein composition of both MFG and casein micelles

356 **Fig. 2-B** (left part) shows the SDS-PAGE patterns corresponding to the protein compositions  
357 of native- or UHT-casein micelles that have been isolated from native- or UHT-skimmed milk  
358 respectively. The protein patterns of native casein micelles corresponded exclusively to  
359 caseins (i.e.  $\alpha$ -,  $\beta$ -,  $\kappa$ -caseins) between 25-37 KDa. In contrast, UHT-casein micelle protein  
360 patterns showed, in addition to caseins, the presence of  $\beta$ -Lg (~18 KDa). Under non-reducing  
361 conditions, the band corresponding to  $\beta$ -Lg and that of  $\kappa$ -caseins were not present in the gel  
362 electrophoresis, indicating that the UHT heat treatment applied to milk induced aggregation of  
363  $\beta$ -Lg with the  $\kappa$ -caseins. This is in agreement with the literature (Anema & Li, 2003a; Donato  
364 & Guyomarc'h, 2009; Vasbinder & de Kruif, 2003).

365 **Fig. 2-B** (right part) shows the SDS-PAGE patterns corresponding to the proteins present at  
366 the surface of MFG in native milk, H-milk and UHT-H-milk. The surface proteins of native-  
367 MFG corresponded exclusively to MFGM proteins, i.e. the xanthine oxidase (154 KDa),  
368 butyrophiline (67 KDa), PAS 6 (50 KDa), PAS 7 (47 KDa) and the mammary derived growth  
369 inhibitor (14 KDa) already described in previous reports (Fong, Norris, & MacGibbon, 2007;  
370 Mather, 2000; Ye, Singh, Taylor, & Anema, 2002; Obeid et al., 2019). In contrast, the surface

371 proteins of H-MFG and UHT-H-MFG, corresponded mainly to caseins. Also, bands  
372 corresponding to  $\beta$ -Lg and  $\alpha$ -La have been identified mainly on the surface UHT-H-MFG and  
373 to a lesser extent (i.e. faint bands) on the surface of unheated H-MFG. Under non-reducing  
374 conditions, the surface protein patterns of UHT-H-MFG were lacking the bands  
375 corresponding to WP, mainly  $\beta$ -Lg, and to  $\kappa$ -casein (**Fig. 2-B**). This result evidenced that  
376 UHT heat treatment induced the formation of complexes between casein micelles and WP  
377 proteins, and that these protein aggregates were adsorbed at the surface of UHT-H-MFG.  
378 These results confirmed i) the adsorption of milk proteins (caseins and WP, mainly  $\beta$ -Lg and  
379  $\alpha$ -La) to the surface of MFG during the homogenization process, and ii) that heat-denaturation  
380 of WP induced by UHT heat treatment favors their co-adsorption with casein micelles onto  
381 the MFG surface (Lee & Sherbon, 2002; Ye, Anema & Singh, 2008).

382 The protein analysis of the particles, MFG and casein micelles, showed that i)  
383 homogenization of milk leads to a partitioning of the casein micelles and the non-denatured  
384 WP between the surface of MFG and the aqueous phase of milk; ii) UHT heat treatment  
385 applied to milk leads to the formation of protein complexes between casein micelles and WP.  
386 These complexes are located both in the aqueous phase of milk and at the surface of  
387 homogenized MFG.

388

### 389 **3.2.2. UHT heat treatment alters the size, the morphology and the $\zeta$ -potential of casein** 390 **micelles**

391 The hydrodynamic diameter  $D_h$  of the native- and UHT-casein micelles was of  $173 \pm 2$  and  
392  $256 \pm 5$  nm, respectively. Therefore, the UHT heat-treatment induced significant increase ( $P <$   
393  $0.001$ ) of the  $D_h$  of casein micelles, by about 80 nm. The morphology and size of the native  
394 casein micelles observed using TEM (**Fig. 2-C**) were in agreement with the literature  
395 (Marchin, Putaux, Pignon, & Léonil, 2007). In contrast, TEM images of UHT-casein micelles  
396 (**Fig. 2-C**) revealed protruding filaments at the surface of casein micelles that may correspond  
397 to the binding of protein aggregates composed of denatured-WP and  $\kappa$ -casein. The colloidal  
398 casein micelle assemblies were therefore affected by UHT heat treatment. This is in  
399 agreement with the early study of Mottar et al. (1989) who showed using electron microscopy  
400 that UHT heat treatment produced long and numerous filaments of denatured-WP at the  
401 casein micelle surface.

402 The  $\zeta$ -potential of casein micelles was affected by UHT heat treatment and by the pH. At pH  
403 6.7, UHT-casein micelles exhibited a significantly lower ( $P < 0.05$ ) negative charge of  $-13.5 \pm$

404 0.7 mV compared to a value of  $-15.6 \pm 0.4$  mV measured for native-casein micelles (**Table 1**).  
405 This was due to the presence of denatured-WP at the UHT-micelle surface (**Fig. 2-C**) ([Anema](#)  
406 [& Klostermeyer, 1996](#); [Donato & Guyomarc'h, 2009](#)). Decreasing the pH from 6.7 down to  
407 4.5 affected the  $\zeta$ -potential values of the casein micelles:  $-2.3 \pm 0.5$  mV for non-heated casein  
408 micelles and  $-2.7 \pm 0.5$  mV for UHT-casein micelles ( $P > 0.05$ ). This decrease in the negative  
409 charge was due to the protonation of the acido-basic groups, e.g. phosphate and carboxylic  
410 residues of casein micelles ([Gaucheron, 2005](#)). The low negative charge of the casein micelles  
411 at acidic pH reduces the electrostatic repulsions between casein micelles and is responsible for  
412 the formation of a protein network in acid gels.

413

### 414 **3.2.3. Homogenization of milk alone or combined with UHT heat treatment alter the size** 415 **and $\zeta$ -potential of fat globules**

416 After homogenization at 20 MPa, H-milk and UHT-H-milk exhibited similar size  
417 distributions of MFG with two major peaks centered at about 0.7 and 0.2  $\mu\text{m}$  (results not  
418 shown). As expected, the small size of MFG in both homogenized milks (below 1  $\mu\text{m}$ )  
419 compared to that of native MFG (4  $\mu\text{m}$ ) was due to the high shear stress applied during the  
420 homogenization process ([Obeid et al., 2019](#); [Lopez, Cauty, & Guyomarc'h, 2015](#); [Michalski](#)  
421 [& Januel, 2006](#)). Homogenization alone or combined with UHT heat treatment of milk did not  
422 induce MFG aggregation. TEM observations of H-milk and UHT-H-milk showed a layer of  
423 proteins adsorbed at the surface of MFG, mainly casein micelles identified due to their  
424 spherical morphology. This is in agreement with the chemical analysis of surface proteins  
425 (**Fig. 2-B**) and previous TEM observations of H-milk ([Obeid et al., 2019](#)).

426 UHT heat treatment of milk significantly ( $P < 0.05$ ) affected the  $\zeta$ -potential values of MFG.  
427 The  $\zeta$ -potential values of MFG were  $-17.3 \pm 0.5$  mV in H-milks and  $-15.4 \pm 0.2$  mV in UHT-  
428 H-milks (**Table 1**). Similarly, the  $\zeta$ -potential of washed MFG prepared for AFM force  
429 spectroscopy experiments was significantly ( $P < 0.05$ ) more negative for washed H-MFG  
430 compared to washed UHT-H-MFG ( $-15.6 \pm 0.9$  mV vs.  $-14.3 \pm 0.5$  mV; **Table 1**). This is due  
431 to the presence of denatured-WP co-adsorbed with casein micelles at the surface of UHT-H-  
432 MFG. These results are in agreement with the difference in  $\zeta$ -potential values that have been  
433 measured between native and UHT-casein micelles (**Table 1**). Decreasing the pH from 6.7  
434 down to 4.5 affected the  $\zeta$ -potential values of the MFG (**Table 1**). At pH 4.5, the negative  $\zeta$ -  
435 potential values of MFG, homogenized or UHT-homogenized, were almost neutralized as a  
436 result of protonation of the acido-basic groups of casein micelles adsorbed at the MFG

437 surface. At acidic pH, the low negative charge of the homogenized MFG reduces the  
438 electrostatic repulsions between MFG (MFG-MFG interactions) and between the MFG and  
439 the surrounding casein micelles. This favors hydrophobic attractive interactions that are the  
440 basis of the building of milk gels.

441

### 442 **3.3. Adhesion forces between homogenized milk fat globules and casein micelles are** 443 **enhanced by acidic pH and UHT heat treatment**

444 AFM topography images of washed and immobilized H-MFG and UHT-H-MFG, recorded in  
445 buffer at pH 6.7, are shown in **Fig. 3-A**. The H-MFG formed a continuous layer of juxtaposed  
446 particles in both samples. Similar AFM topography images were obtained upon acidification  
447 to pH 4.5 (results not shown).

448 **Fig. 3-B, D** show examples of adhesion force maps measured between the casein micelles-  
449 modified AFM probes and immobilized H-MFG or UHT-H-MFG, at pH 6.7 and pH 4.5. The  
450 measured adhesion forces,  $F_{adh}$  values, ranged from few pN to few nN. Force curves showing  
451 no adhesive events (below 45 pN) are represented as dark-blue pixels in the force maps. The  
452 percentage of force curves showing significant adhesion events was of 47 and 57 % for the  
453 adhesion between native casein micelles and H-MFG at pH 6.7 and 4.5, respectively. This  
454 percentage was significantly higher between UHT-casein micelles and UHT-H-MFG than  
455 between their unheated counterparts, with values of 71 and 94 % at pH 6.7 and 4.5,  
456 respectively. The adhesion forces increased upon acidification to pH 4.5 in both experimental  
457 set-ups as evidenced by the increase in the proportion of green and orange pixels in the force  
458 maps recorded at pH 4.5 (**Fig. 3-D**) compared to those measured at pH 6.7 (**Fig. 3-B**).

459 The retraction force curves showed adhesion events between the casein micelles grafted on  
460 the AFM probes and the H-MFG or the UHT-H-MFG, at pH 6.7 (**Fig. 3-C**) and at pH 4.5  
461 (**Fig. 3-E**). The adhesion events were successfully fitted with the Worm-Like Chain (WLC)  
462 model that describes the mechanical stretching response of polypeptides under a pulling force,  
463 with supplementary insights on the flexibility of molecules during multiple interactions which  
464 is likely to occur when using colloidal probes (Friedrichs et al., 2013; Marszalek & Dufrêne,  
465 2012; Francius et al., 2009; Obeid et al., 2019). The adhesion events were therefore the  
466 signature of the stretching of polypeptides molecules, i.e. the casein micelles alone or coated  
467 with heat-denatured WP, located both at the surface of MFG or grafted on the AFM probes.  
468 This is in agreement with our previous study on adhesion forces between homogenized  
469 casein-coated MFG and casein micelles (Obeid et al., 2019).



470 From the retraction force curves, the adhesion forces  $F_{adh}$  and the maximal rupture distance  
471  $D_{adh}$  were analyzed as described in **Fig. 1-C**. The median  $F_{adh}$  between unheated casein  
472 micelles and unheated H-MFG increased nearly 1.4 fold, from 125 pN at pH 6.7 to 176 pN at  
473 pH 4.5 ( $P < 0.001$ ; **Fig. 4-A**). Meanwhile, the median  $F_{adh}$  between UHT-casein micelles and  
474 UHT-H-MFG increased about 3.5 fold, from 85 pN at pH 6.7 to 296 pN at pH 4.5 ( $P < 0.001$ ;  
475 **Fig. 4-A**). Concomitantly, the maximal rupture distance ( $D_{adh}$ ) also increased significantly ( $P$   
476  $< 0.001$ ) upon acidification of the experimental media in both unheated and UHT conditions  
477 (**Fig. 4-B**). Such an increase in  $F_{adh}$  and  $D_{adh}$  values upon acidification is in agreement with  
478 previous results obtained with native MFG and homogenized MFG (Obeid et al., 2019). This  
479 increase in  $D_{adh}$  when pH is decreased should be related to stronger attractive interaction and  
480 less electrostatic repulsive forced between the components present at the surface of MFG and  
481 the proteins grafted on the AFM probe. Furthermore, for each pH condition, the  $D_{adh}$  was  
482 shorter between UHT-casein micelles and UHT-H-MFG than between unheated casein  
483 micelles and unheated H-MFG. At pH 4.5 for instance, the median  $D_{adh}$  were respectively 110  
484 and 151 nm (**Fig. 4-B**;  $P < 0.001$ ). Furthermore, only at pH 6.7, the median  $F_{adh}$  between  
485 unheated casein micelles and unheated H-MFG was significantly higher (125 pN) than that  
486 between UHT-casein micelles and UHT-H-MFG (85 pN (**Fig. 4-A**), even though the  
487 percentage of adhesive events was lower in the first case (47% vs. 71% respectively).

488

### 489 **3.4. Microstructure and acid gelation behavior of the milks as a function of pH**

490 The CLSM observations performed at neutral pH showed that the MFG and milk proteins in  
491 both H-milk and UHT-H-milk samples were homogeneously dispersed in the aqueous phase  
492 (**Fig. 5**). This results from the electrostatic repulsion between the negatively charged  
493 homogenized MFG and the casein micelles (**Table 1**). CLSM observations performed after  
494 acidification of milk samples to pH 4.5 (**Fig. 5**) showed in both samples that the casein  
495 micelles aggregated and formed a protein network where the MFG were fully entrapped, as  
496 the result of the presence of casein micelles adsorbed on their surface (**Fig. 2 B**). This is in  
497 agreement with previous CLSM observations of acid homogenized milk gels (Lopez, Cauty &  
498 Guyomarc'h, 2015; Michalski et al., 2002; Obeid et al., 2019). Moreover, **Fig. 5** shows that  
499 the acid gels formed by H-milk displayed clustered network, while that formed by UHT-H-  
500 milk showed more branched network with higher connectivity. This is in agreement with the  
501 literature (Kalab, Emmons, & Sargent, 1975; Lucey, Munro, & Singh, 1998). As a conclusion,

502 the UHT heat treatment of milk affected the microstructure of the milk acid gels as compared  
503 to unheated H-milk.

504 Rheological measurements were performed as a function of the decrease in pH in both H-milk  
505 and UHT-H-milk (**Fig. 6**). The transition from liquid to gel state was obtained when the  
506 storage modulus  $G'$  became higher than the loss modulus  $G''$  (results not shown). The pH of  
507 H-milk decreased more slowly compared to that of UHT-H-milk. The time necessary to reach  
508 the gelation pH was of  $24.3 \pm 1.6$  and of  $6.4 \pm 0.6$  min for H-milk and UHT-H-milks,  
509 respectively. In addition, the gelation pH was significantly ( $P < 0.001$ ) lower for H-milk (pH  
510 =  $4.9 \pm 0.1$ ) compared to UHT-H-milk (pH =  $5.2 \pm 0.1$ ). This is in agreement with previous  
511 studies showing that the presence of heat-denatured WP/ $\kappa$ -casein aggregates increases the  
512 gelation pH from about 4.9 to 5.1-5.3 and decreases the gelation time of skimmed milk acid  
513 gels (Krasaekoopt, Bhandari, & Deeth, 2003). In addition, the final  $G'$  value of milk acid gels  
514 at pH 4.5 was about 7 fold higher in UHT-H-milk gels compared to H-milk gels ( $136.2 \pm 12.7$   
515 Pa vs.  $18.7 \pm 2.8$  Pa;  $P < 0.001$ ; **Fig. 6**). As a conclusion, the UHT heat-treatment of  
516 homogenized milk increased the stiffness of the acid gels as compared to non-heated  
517 homogenized milk, which is consistent with previous studies (Guyomarc'h, Queguiner, Law,  
518 Horne, & Dalgleish, 2003; Krasaekoopt et al., 2003; Lucey & Singh, 1997).

519

### 520 **3.5. Impact of milk heat treatment and pH: multiscale link between surface properties of** 521 **homogenized MFG and casein micelles, nanoscale adhesion forces, microstructure** 522 **and rheological properties**

523 In this study, we showed that the process-induced changes in the surface properties of MFG  
524 and casein micelles were markedly sensitive to the pH (**Table 1**) with consequences on the  
525 adhesion between particles (**Fig. 3 and 4**), on the microstructure (**Fig. 5**) and on the  
526 rheological properties of milk acid gels (**Fig. 6**), as summarized **Figure 7**. These results  
527 require further discussions.

528 At neutral pH, both the casein micelles and protein-coated homogenized MFG were  
529 negatively charged in H-milks and UHT-H-milks (**Table 1**). Thus, under physiological  
530 conditions, electrostatic repulsions prevented contact between homogenized MFG and the  
531 casein micelles located in the surrounding aqueous phase, as shown in confocal images (**Fig.**  
532 **5**). However, in our AFM force spectroscopy experiments, casein micelles grafted on the  
533 AFM probe and immobilized homogenized MFG were forced into contact during the

534 recording of approach curves (**Fig 1-A**). In the absence of UHT heat treatment, a median  
535 adhesion force  $F_{adh}$  of 125 pN occurred between native casein micelles, either attached to the  
536 AFM probes or covering the surface of H-MFG (**Fig. 4-A**). Native casein micelles are flexible  
537 assemblies with low secondary and tertiary structures (Holt, Carver, Ecroyd, & Thorn, 2013).  
538 Once in contact, they interact through hydrogen bonds, hydrophobic and van der Waals  
539 interactions and can rearrange up to optimized interaction (Dalglish, 2011). In absence of  
540 heat treatment, native WP do not contribute to this caseins – caseins interaction (Lucey,  
541 Munro, & Singh, 1999). When the milks were UHT heat-treated before homogenization, the  
542 adhesion forces involved UHT-casein micelles with denatured-WP aggregates attached to  
543 their surface both grafted on the AFM probe and adsorbed at the surface of MFG (**Fig. 1-A &**  
544 **2-C**). The  $\zeta$ -potential measurements showed a decrease in the negative value (**Table 1**) due to  
545 the adsorption of WP induced by UHT heat treatment. Denatured-WP were therefore  
546 responsible of the significant ( $P < 0.001$ ) decrease in the median adhesion forces  $F_{adh}$  from  
547 125 pN to 85 pN (**Fig. 4-A**). The denatured-WP aggregates protruding from the casein micelle  
548 surface (**Fig. 2-C**) have been reported to decrease the flexibility (i.e. deformability) of the  
549 UHT-casein micelles (Donato & Guyomarc'h, 2009). This may be responsible for the  
550 decrease in the  $F_{adh}$  and  $D_{adh}$  measured between UHT-casein micelles and UHT-H-MFG at pH  
551 6.7 compared to the same parameters measured during adhesion between native-casein  
552 micelles and H-MFG. Therefore, at pH 6.5-6.7, the presence of denatured-WP aggregates at  
553 the surface of the casein micelles in UHT samples somewhat further prevented adhesion  
554 between individual casein micelles, already stabilized by electrostatic and steric repulsions.

555 At acidic pH of 4.5, the low negative charges of casein micelles, WP aggregates and  
556 homogenized MFG, with or without UHT heat treatment (**Table 1**), lead to a reduction in the  
557 electrostatic repulsion between these components. In addition, casein micelles undergo  
558 several changes upon acidification to pH 4.5 mainly demineralization and the collapse of their  
559  $\kappa$ -casein hairy layer (Gaucheron, 2005). The formation of a protein network in which  
560 homogenized MFG were entrapped in the casein strands was observed in CLSM images, with  
561 stranded protein structures due to high hydrophobic interactions between denatured-WP in the  
562 UHT-H-milk gel (**Fig. 5**). AFM experiments showed that the adhesion forces  $F_{adh}$  between  
563 casein micelles and homogenized MFG significantly ( $P < 0.001$ ) increased upon acidification  
564 in unheated samples (from 125 pN to 176 pN; 1.4-fold) and UHT heat-treated samples (from  
565 85 pN to 296 pN; 3.5-fold) (**Fig. 4-A**). The denatured-WP aggregates present both at the  
566 surface of the UHT-casein micelles and adsorbed at the surface of UHT-H-MFG enhance the

567 surface hydrophobicity and increase the number of adhesive sites on the surface of UHT-  
568 casein micelles (Donato & Guyomarc'h, 2009; Jean, Renan, Famelart, & Guyomarc'h, 2006).  
569 The denatured-WP aggregates are responsible for significantly ( $P < 0.001$ ) higher adhesion  
570 forces measured between UHT-casein micelles grafted on the AFM probes and on the UHT-  
571 H-MFG (median  $F_{adh} = 296$  pN), compared to the adhesion between native casein micelles  
572 and H-MFG (median  $F_{adh} = 176$  pN) (**Fig. 4-A**). The results obtained at the individual particle  
573 level were coherent with rheological properties measured at the macroscopic scale, where the  
574  $G'$  value recorded at pH 4.5 for UHT heat-treated homogenized milk was significantly ( $P <$   
575  $0.001$ ) higher than that of the unheated homogenized milk (**Fig. 6**). These results obtained at  
576 the nanoscale highlight the role of inter-particle interactions in the building of the macroscale  
577 rheological properties of the acid milk gels (**Fig. 7**). In a pioneer work, Uricanu et al. (2004)  
578 evidenced that the  $G'$  value of individual casein micelles, measured by AFM indentation, did  
579 not significantly vary as a function of pH. From this, they hypothesized that inter-particle  
580 interactions, rather than intra-particle ones, were responsible for the macroscopic texture of  
581 the acid milk gels. Our results now bring positive evidence to support this assumption, and  
582 show that measurement of particle-particle adhesion force at the nanoscale is predictive of the  
583 bulk texture of acid milk gels.

584 From a methodological point of view, this study and the previous one (Obeid et al., 2019)  
585 showed that AFM force spectroscopy provides new quantitative information into the  
586 interaction between individual MFG and proteins at the nanoscale level which govern at the  
587 macroscale level the microstructure and rheological properties of dairy acid gels. This work  
588 clarifies in light of science the assumptions made in the last decade about the physicochemical  
589 interactions between lipids and proteins in a complex food system such as milk. Also, this  
590 work opens new perspectives for a better understanding of the effect of the interfacial  
591 compositions on the pair-pair interactions between individual food objects that is involved in  
592 food product quality.

593

#### 594 **4. Conclusion**

595 Full understanding of how technological processes impact the interactions between particles,  
596 e.g. lipid-protein or protein-protein interactions, that contribute to the microstructure and  
597 rheology of food products require further knowledge. In this paper, we studied for the first  
598 time at the nanoscale level the effect of UHT heat treatment of milk on the interactions  
599 between individual homogenized MFG and casein micelles, using AFM force spectroscopy.

600 We showed that homogenized MFG interact with the surrounding proteins at acidic pH and  
601 that they are active fillers in a protein network. UHT heat treatment of milk increased the  
602 adhesion forces measured at pH 4.5 between protein-coated homogenized MFG and the  
603 proteins grafted on AFM probes. This was due to the presence of highly reactive heat-  
604 denatured WP attached to the casein micelles. Denatured-WP in UHT-homogenized milks  
605 ensures higher hydrophobic adhesion forces i) between casein micelles in the protein strands  
606 forming the acid gel, and ii) between the casein micelles adsorbed at the surface of H-MFG  
607 and those in the protein network. This leads to the formation of highly connected and stiffer  
608 UHT heat-treated acid gels compared to that formed by unheated homogenized-milks. This  
609 study provides new quantitative information at the nanoscale level through AFM force  
610 spectroscopy on the effect of technological processes (homogenization, heat treatment,  
611 acidification). Such findings will be useful for the dairy industry to modulate the texture of  
612 fermented dairy products, for example yoghurts, through the tailoring of heat-induced  
613 complexation of proteins and the connectivity of homogenized MFG with the protein  
614 network.

615

## 616 **Acknowledgements**

617 Sameh Obeid's postdoctoral fellowship was funded by CNIEL (French Dairy Interbranch  
618 Organization, Paris, France) in the Moon project (scientific coord. C. Lopez, INRA). The  
619 authors thank all the members of CNIEL's committee on dairy lipids for stimulating  
620 discussions about milk fat globules and dairy processing. Christelle Lopez warmly thanks Mr  
621 and Mrs Denoual from Gaec des Fougères for providing milk samples. The authors are  
622 grateful to the INRA STLO Platform ([https://www6.rennes.inra.fr/plateforme\\_lait](https://www6.rennes.inra.fr/plateforme_lait)).  
623 Maryvonne Pasco and Jordane Ossemond (INRA-STLO, Rennes) are acknowledged for their  
624 contribution in gel-electrophoresis analysis of MFG surface proteins and CLSM observations  
625 of AFM tips, respectively. Grégory Francius (LCPME, CNRS, Nancy, France) and Jennifer  
626 Burgain (LIBio, Université de Lorraine, Nancy, France) are thanked for useful advice on  
627 analysis of AFM retraction force curves using the WLC model and on AFM colloidal probes,  
628 respectively. TEM images were taken at the Microscopy Rennes Imaging Center (University  
629 Rennes 1, France). The Asylum Research MFP3D-BIO atomic force microscope was funded  
630 by the European Union (FEDER), the French Ministry of Education and Research, INRA,  
631 Conseil Général 35 and Rennes Métropole.

632

633 **References**

- 634 Ahmad, S., Gaucher, I., Rousseau, F., Beaucher, E., Piot, M., Grongnet, J. F., & Gaucheron,  
635 F. (2008). Effects of acidification on physico-chemical characteristics of buffalo milk: A  
636 comparison with cow's milk. *Food Chemistry*, *106*(1), 11–17.  
637 <https://doi.org/10.1016/j.foodchem.2007.04.021>
- 638 Anema, S. G., & Klostermeyer, H. (1996).  $\zeta$ -Potentials of casein micelles from reconstituted  
639 skim milk heated at 120 °C. *International Dairy Journal*, *6*(7), 673–687.  
640 [https://doi.org/10.1016/0958-6946\(95\)00070-4](https://doi.org/10.1016/0958-6946(95)00070-4)
- 641 Anema, S. G., & Li, Y. (2003a). Association of denatured whey proteins with casein micelles  
642 in heated reconstituted skim milk and its effect on casein micelle size. *Journal of Dairy*  
643 *Research*, *70*(1), 73–83. <https://doi.org/10.1017/S0022029902005903>
- 644 Anema, S. G., & Li, Y. (2003b). Effect of pH on the association of denatured whey proteins  
645 with casein micelles in heated reconstituted skim milk. *Journal of Agricultural and Food*  
646 *Chemistry*, *51*(6), 1640–1646. <https://doi.org/10.1021/jf025673a>
- 647 Anema, S. G., & McKenna, A. B. (1996). Reaction Kinetics of Thermal Denaturation of  
648 Whey Proteins in Heated Reconstituted Whole Milk. *Journal of Agricultural and Food*  
649 *Chemistry*, *44*(2), 422–428. <https://doi.org/10.1021/jf950217q>
- 650 Dalgleish, D. G. (2011). On the structural models of bovine casein micelles—review and  
651 possible improvements. *Soft Matter*, *7*(6), 2265–2272. <https://doi.org/10.1039/C0SM00806K>
- 652 Donato, L., & Guyomarc'h, F. (2009). Formation and properties of the whey protein/ $\kappa$ -casein  
653 complexes in heated skim milk — A review. *Dairy Science and Technology*, *89*, 3–29.  
654 <https://doi.org/10.1051/dst:2008033>
- 655 Farrell, H. M., Jimenez-Flores, R., Bleck, G. T., Brown, E. M., Butler, J. E., Creamer, L. K.,  
656 ... Swaisgood, H. E. (2004). Nomenclature of the proteins of cows' milk—Sixth revision.  
657 *Journal of Dairy Science*, *87*(6), 1641–1674. [https://doi.org/10.3168/jds.S0022-0302\(04\)73319-6](https://doi.org/10.3168/jds.S0022-0302(04)73319-6)
- 659 Fong, B. Y., Norris, C. S., & MacGibbon, A. K. H. (2007). Protein and lipid composition of  
660 bovine milk-fat-globule membrane. *International Dairy Journal*. Retrieved from  
661 <http://agris.fao.org/agris-search/search.do?recordID=US201300756275>
- 662 Francius, G., Alsteens, D., Dupres, V., Lebeer, S., De Keersmaecker, S., Vanderleyden, J., ...  
663 Dufrière, Y. F. (2009). Stretching polysaccharides on live cells using single molecule force  
664 spectroscopy. *Nature Protocols*, *4*(6), 939–946. <https://doi.org/10.1038/nprot.2009.65>
- 665 Friedrichs, J., Legate, K. R., Schubert, R., Bharadwaj, M., Werner, C., Müller, D. J., &  
666 Benoit, M. (2013). A practical guide to quantify cell adhesion using single-cell force  
667 spectroscopy. *Methods*, *60*(2), 169–178. <https://doi.org/10.1016/j.ymeth.2013.01.006>
- 668 Garcia, C., Antona, C., Robert, B., Lopez, C., & Armand, M. (2014). The size and interfacial  
669 composition of milk fat globules are key factors controlling triglycerides bioavailability in  
670 simulated human gastro-duodenal digestion. *Food Hydrocolloids*, *35*, 494–504.  
671 [doi:10.1016/j.foodhyd.2013.07.005](https://doi.org/10.1016/j.foodhyd.2013.07.005).

- 672 García-Risco, M. R., Ramos, M., & López-Fandiño, R. (2002). Modifications in milk proteins  
673 induced by heat treatment and homogenization and their influence on susceptibility to  
674 proteolysis. *International Dairy Journal*, 12(8), 679–688. [https://doi.org/10.1016/S0958-6946\(02\)00060-2](https://doi.org/10.1016/S0958-6946(02)00060-2)  
675
- 676 Gaucheron, F. (2005). The minerals of milk. *Reproduction Nutrition Development*, 45(4),  
677 473–483. <https://doi.org/10.1051/rnd:2005030>
- 678 Gunning, A. P., & Morris, V. J. (2018). Getting the feel of food structure with atomic force  
679 microscopy. *Food Hydrocolloids*, 78, 62–76. <https://doi.org/10.1016/j.foodhyd.2017.05.017>
- 680 Guyomarc'h, F., Queguiner, C., Law, A. J. R., Horne, D. S., & Dalgleish, D. G. (2003). Role  
681 of the Soluble and Micelle-Bound Heat-Induced Protein Aggregates on Network Formation in  
682 Acid Skim Milk Gels. *Journal of Agricultural and Food Chemistry*, 51(26), 7743–7750.  
683 <https://doi.org/10.1021/jf030201x>
- 684 Holt, C., Carver, J. A., Ecroyd, H., & Thorn, D. C. (2013). Invited review: Caseins and the  
685 casein micelle: Their biological functions, structures, and behavior in foods. *Journal of Dairy  
686 Science*, 96(10), 6127–6146. <https://doi.org/10.3168/jds.2013-6831>
- 687 IDF Standard 20B:1993: Milk: Determination of Nitrogen Content: Inspection by Attributes.  
688 (1993). IDF.
- 689 ISO 8968-1: Milk and milk products - Determination of nitrogen content - Part 1: Kjeldahl  
690 principle and crude protein calculation. (2014). Retrieved February 13, 2019, from  
691 <https://www.iso.org/obp/ui/#iso:std:iso:8968:-1:ed-2:v1:en>
- 692 ISO 8968-4: Milk and milk products - Determination of nitrogen content - Part 4:  
693 Determination of protein and non-protein nitrogen content and true protein content calculation  
694 (Reference method). (2016). Retrieved February 13, 2019, from  
695 <http://www.iso.org/cms/render/live/fr/sites/isoorg/contents/data/standard/06/03/60386.html>
- 696 ISO 17997-1: Determination of casein-nitrogen content - Part 1: Indirect method (Reference  
697 method). (2004). Retrieved February 13, 2019, from ISO website:  
698 <http://www.iso.org/cms/render/live/fr/sites/isoorg/contents/data/standard/03/16/31670.html>
- 699 Jean, K., Renan, M., Famelart, M.-H., & Guyomarc'h, F. (2006). Structure and surface  
700 properties of the serum heat-induced protein aggregates isolated from heated skim milk.  
701 *International Dairy Journal*, 16(4), 303–315. <https://doi.org/10.1016/j.idairyj.2005.04.001>
- 702 Jukkola, A., & Rojas, O.J. (2017). Milk fat globules and associated membranes: Colloidal  
703 properties and processing effects. *Advances in Colloid and Interface Science*, 245, 92–101.  
704 <http://dx.doi.org/10.1016/j.cis.2017.04.010>
- 705 Kalab, M., B. Emmons, D., & G. Sargent, A. (1975). Milk gel structure. IV. Microstructure of  
706 yoghurts in relation to the presence of thickening agents. *Journal of Dairy Research*, 42, 453–  
707 458. <https://doi.org/10.1017/S0022029900015491>
- 708 Karman, A. H., & Van Boekel, M. A. J. S. (1986). Evaluation of the Kjeldahl factor for  
709 conversion of the nitrogen content of milk and milk products to protein content. *Netherlands  
710 Milk and Dairy Journal (Netherlands)*. Retrieved from [http://agris.fao.org/agris-  
711 search/search.do?recordID=NL8700834](http://agris.fao.org/agris-search/search.do?recordID=NL8700834)

- 712 Krasaekoopt, W., Bhandari, B., & Deeth, H. C. (2003). Yogurt from UHT milk: A review.  
713 *Australian Journal of Dairy Technology*, 58(1), 26–29.
- 714 Le, D. T. L., Tran, T.-L., Duviau, M.-P., Meyrand, M., Guérardel, Y., Castelain, M., ...  
715 Mercier-Bonin, M. (2013). Unraveling the Role of Surface Mucus-Binding Protein and Pili in  
716 Muco-Adhesion of *Lactococcus lactis*. *PLOS ONE*, 8(11), e79850.  
717 <https://doi.org/10.1371/journal.pone.0079850>
- 718 Lee, S. J., & Sherbon, J. W. (2002). Chemical changes in bovine milk fat globule membrane  
719 caused by heat treatment and homogenization of whole milk. *The Journal of Dairy Research*,  
720 69(4), 555–567.
- 721 Lévy, R., & Maaloum, M. (2001). Measuring the spring constant of atomic force microscope  
722 cantilevers: Thermal fluctuations and other methods. *Nanotechnology*, 13(1), 33–37.  
723 <https://doi.org/10.1088/0957-4484/13/1/307>
- 724 Liang, L., Qi, C., Wang, X., Jin, Q., & McClements, D.J. (2017). Influence of  
725 Homogenization and Thermal Processing on the Gastrointestinal Fate of Bovine Milk Fat: In  
726 Vitro Digestion Study. *J. Agric. Food Chem.* 65, 11109–11117.  
727 <https://doi.org/10.1021/acs.jafc.7b04721>
- 728 Lopez, C., & Dufour, E. (2001). The Composition of the Milk Fat Globule Surface Alters the  
729 Structural Characteristics of the Coagulum. *Journal of Colloid and Interface Science*, 233(2),  
730 241–249. <https://doi.org/10.1006/jcis.2000.7255>
- 731 Lopez, C. (2011). Milk fat globules enveloped by their biological membrane: Unique  
732 colloidal assemblies with a specific composition and structure. *Current Opinion in Colloid &*  
733 *Interface Science*, 16(5), 391–404. <https://doi.org/10.1016/j.cocis.2011.05.007>
- 734 Lopez, C., Cauty, C., & Guyomarc'h, F. (2015). Organization of lipids in milks, infant milk  
735 formulas and various dairy products: Role of technological processes and potential impacts.  
736 *Dairy Science & Technology*, 95(6), 863–893. <https://doi.org/10.1007/s13594-015-0263-0>
- 737 Lucey, J. A., Munro, P. A., & Singh, H. (1998). Rheological Properties and Microstructure of  
738 Acid Milk Gels as Affected by Fat Content and Heat Treatment. *Journal of Food Science*,  
739 63(4), 660–664. <https://doi.org/10.1111/j.1365-2621.1998.tb15807.x>
- 740 Lucey, J. A., Munro, P. A., & Singh, H. (1999). Effects of heat treatment and whey protein  
741 addition on the rheological properties and structure of acid skim milk gels. *International*  
742 *Dairy Journal*, 9(3), 275–279. [https://doi.org/10.1016/S0958-6946\(99\)00074-6](https://doi.org/10.1016/S0958-6946(99)00074-6)
- 743 Lucey, J. A., & Singh, H. (1997). Formation and physical properties of acid milk gels: A  
744 review. *Food Research International*, 30(7), 529–542. [https://doi.org/10.1016/S0963-](https://doi.org/10.1016/S0963-9969(98)00015-5)  
745 [9969\(98\)00015-5](https://doi.org/10.1016/S0963-9969(98)00015-5)
- 746 Marchin, S., Putaux, J.-L., Pignon, F., & Léonil, J. (2007). Effects of the environmental  
747 factors on the casein micelle structure studied by cryo transmission electron microscopy and  
748 small-angle x-ray scattering/ultras-small-angle x-ray scattering. *The Journal of Chemical*  
749 *Physics*, 126(4), 045101. <https://doi.org/10.1063/1.2409933>
- 750 Marszalek, P. E., & Dufrêne, Y. F. (2012). Stretching single polysaccharides and proteins  
751 using atomic force microscopy. *Chemical Society Reviews*, 41(9), 3523–3534.



- 752 <https://doi.org/10.1039/c2cs15329g>
- 753 Mather, I. H. (2000). A Review: Proposed Nomenclature for Major Proteins of the Milk-Fat  
754 Globule Membrane. *Journal of Dairy Science*, 83(2), 203–247.  
755 [https://doi.org/10.3168/jds.S0022-0302\(00\)74870-3](https://doi.org/10.3168/jds.S0022-0302(00)74870-3)
- 756 Michalski, M. C., Cariou, R., Michel, F., & Garnier, C. (2002). Native vs. Damaged Milk Fat  
757 Globules: Membrane Properties Affect the Viscoelasticity of Milk Gels. *Journal of Dairy*  
758 *Science*, 85(10), 2451–2461. [https://doi.org/10.3168/jds.S0022-0302\(02\)74327-0](https://doi.org/10.3168/jds.S0022-0302(02)74327-0)
- 759 Michalski, M.-C., & Januel, C. (2006). Does homogenization affect the human health  
760 properties of cow's milk? *Trends in Food Science & Technology*, 17(8), 423–437.  
761 <https://doi.org/10.1016/j.tifs.2006.02.004>
- 762 Morand, M., Dekkari, A., Guyomarc'h, F., & Famelart, M.-H. (2012). Increasing the  
763 hydrophobicity of the heat-induced whey protein complexes improves the acid gelation of  
764 skim milk. *International Dairy Journal*, 25(2), 103–111.  
765 <https://doi.org/10.1016/j.idairyj.2012.03.002>
- 766 Mottar, J., Bassier, A., Joniau, M., & Baert, J. (1989). Effect of Heat-Induced Association of  
767 Whey Proteins and Casein Micelles on Yogurt Texture. *Journal of Dairy Science*, 72(9),  
768 2247–2256. [https://doi.org/10.3168/jds.S0022-0302\(89\)79355-3](https://doi.org/10.3168/jds.S0022-0302(89)79355-3)
- 769 Mulet-Cabero, A.-I., Mackie, A.R., Wilde, P.J., Fenelon, M.A., and Brodkorb, A. (2019).  
770 Structural mechanism and kinetics of in vitro gastric digestion are affected by process-  
771 induced changes in bovine milk. *Food Hydrocolloids* 86, 172–183.  
772 <https://doi.org/10.1016/j.foodhyd.2018.03.035>
- 773 Müller, D. J., Krieg, M., Alsteens, D., & Dufrêne, Y. F. (2009). New frontiers in atomic force  
774 microscopy: Analyzing interactions from single-molecules to cells. *Current Opinion in*  
775 *Biotechnology*, 20(1), 4–13. <https://doi.org/10.1016/j.copbio.2009.02.005>
- 776 Obeid, S., Guyomarc'h, F., Francius, G., Guillemain, H., Wu, X., Pezenec, S., ... Lopez, C.  
777 (2019). The surface properties of milk fat globules govern their interactions with the caseins:  
778 Role of homogenization and pH probed by AFM force spectroscopy. *Colloids and Surfaces*  
779 *B: Biointerfaces*, 182, 110363. <https://doi.org/10.1016/j.colsurfb.2019.110363>
- 780 Oldfield, D. J., Singh, H., Taylor, M. W., & Pearce, K. N. (1998). Kinetics of Denaturation  
781 and Aggregation of Whey Proteins in Skim Milk Heated in an Ultra-high Temperature (UHT)  
782 Pilot Plant. *International Dairy Journal*, 8(4), 311–318. [https://doi.org/10.1016/S0958-6946\(98\)00089-2](https://doi.org/10.1016/S0958-6946(98)00089-2)
- 784 Patton, S., & Huston, G. E. (1986). A method for isolation of milk fat globules. *Lipids*, 21(2),  
785 170–174. <https://doi.org/10.1007/BF02534441>
- 786 Renan, M., Guyomarc'h, F., Chatriot, M., Gamerre, V., & Famelart, M.-H. (2007). Limited  
787 Enzymatic Treatment of Skim Milk Using Chymosin Affects the Micelle/Serum Distribution  
788 of the Heat-Induced Whey Protein/ $\kappa$ -Casein Aggregates. *Journal of Agricultural and Food*  
789 *Chemistry*, 55(16), 6736–6745. <https://doi.org/10.1021/jf0705771>
- 790 Tuinier, R., & de Kruif, C. G. (2002). Stability of casein micelles in milk. *The Journal of*  
791 *Chemical Physics*, 117(3), 1290–1295. <https://doi.org/10.1063/1.1484379>

- 792 Uricanu, V. I., Duits, M. H. G., & Mellema, J. (2004). Hierarchical networks of casein  
793 proteins: An elasticity study based on atomic force microscopy. *Langmuir: The ACS Journal*  
794 *of Surfaces and Colloids*, 20(12), 5079–5090.
- 795 van Vliet, T. (1988). Rheological properties of filled gels. Influence of filler matrix  
796 interaction. *Colloid and Polymer Science*, 266(6), 518–524.  
797 <https://doi.org/10.1007/BF01420762>
- 798 Vasbinder, A. J., & de Kruif, C. G. (2003). Casein–whey protein interactions in heated milk:  
799 The influence of pH. *International Dairy Journal*, 13(8), 669–677.  
800 [https://doi.org/10.1016/S0958-6946\(03\)00120-1](https://doi.org/10.1016/S0958-6946(03)00120-1)
- 801 West, R., & Rousseau, D. (2018). The role of nonfat ingredients on confectionery fat  
802 crystallization. *Critical Reviews in Food Science and Nutrition*, 58(11), 1917–1936.  
803 <https://doi.org/10.1080/10408398.2017.1286293>
- 804 Ye, A., Anema, S. G., & Singh, H. (2008). Changes in the surface protein of the fat globules  
805 during homogenization and heat treatment of concentrated milk. *The Journal of Dairy*  
806 *Research*, 75(3), 347–353. <https://doi.org/10.1017/S0022029908003464>
- 807 Ye, A., Singh, H., Taylor, M. W., & Anema, S. (2002). Characterization of protein  
808 components of natural and heat-treated milk fat globule membranes. *International Dairy*  
809 *Journal*, 12(4), 393–402. [https://doi.org/10.1016/S0958-6946\(02\)00034-1](https://doi.org/10.1016/S0958-6946(02)00034-1)
- 810 Ye, A., Cui, J., Dalgleish, D., and Singh, H. (2017). Effect of homogenization and heat  
811 treatment on the behavior of protein and fat globules during gastric digestion of milk. *Journal*  
812 *of Dairy Science* 100, 36–47. <https://doi.org/10.3168/jds.2016-11764>
- 813 Zhao, L., Du, M., & Mao, X. (2019). Change in interfacial properties of milk fat globules by  
814 homogenization and thermal processing plays a key role in their in vitro gastrointestinal  
815 digestion. *Food Hydrocolloids* 96, 331–342. <https://doi.org/10.1016/j.foodhyd.2019.05.034>
- 816

817 **Table**

818

819 **Table 1.** Zeta-potential values of milk fat globules (MFG) and casein micelles after milk  
 820 homogenization (H) at 20 MPa, or after ultra-high temperature (UHT) heat treatment  
 821 combined with homogenization at 20 MPa. The zeta-potential values have been determined at  
 822 pH 6.7 and 4.5 in milk and in samples of washed MFG or casein micelles isolated from milk.  
 823 ND: non-determined due to the precipitation of caseins.

| Samples                       | $\zeta$ -potential (mV) |                |
|-------------------------------|-------------------------|----------------|
|                               | pH 6.7                  | pH 4.5         |
| <b>H-milk</b>                 | $-17.3 \pm 0.5^*$       | ND             |
| <b>UHT-H-milk</b>             | $-15.4 \pm 0.2^*$       | ND             |
| <b>Washed H-MFG</b>           | $-15.6 \pm 0.9^{**}$    | $-4.7 \pm 0.6$ |
| <b>Washed UHT-H-MFG</b>       | $-14.3 \pm 0.5^{**}$    | $-4.0 \pm 0.5$ |
| <b>Native-casein micelles</b> | $-15.6 \pm 0.4^{***}$   | $-2.3 \pm 0.5$ |
| <b>UHT-casein micelles</b>    | $-13.5 \pm 0.7^{***}$   | $-2.7 \pm 0.5$ |

824 Mean values calculated from 3 independent experiments. Analysis of variance: \*, \*\*, \*\*\*  
 825 indicate significant differences with  $P < 0.05$ .

826

827

828 **Figure caption**

829

830 **Fig. 1.** (A) Schematic illustration, not to scale, of the AFM force spectroscopy experiments  
831 performed to measure the adhesion forces between casein micelles grafted to the AFM probes  
832 and homogenized milk fat globules (MFG) immobilized on filter membranes. The casein  
833 micelles and MFG were isolated from milks that have been either homogenized or heat  
834 treated at ultra-high temperature (UHT) and homogenized. AFM measurements were  
835 performed in PIPES buffer at 22°C. (B) Confocal laser scanning microscopy image showing  
836 fluorescently-labelled caseins successfully grafted on the AFM probe. (C) Example of AFM  
837 force curves where the maximal adhesion force  $F_{adh}$  and rupture distance  $D_{adh}$  are determined  
838 from the retraction curve.

839 **Fig. 2.** Chemical analysis and morphology of proteins. (A) Relative percentage of of milk  
840 proteins: caseins, native whey proteins (WP) or heat-denatured-WP in native milk, native  
841 skimmed milk, homogenized (H-) milk, and samples of milks after heat treatment at ultra-  
842 high temperature (UHT). (B) SDS-Page patterns of isolated native and UHT-casein micelles  
843 (CM) and of the interfacial proteins adsorbed on native-MFG, H-MFG and UHT-H-MFG. (\*)  
844 indicates electrophoresis under non-reducing conditions. (C) Transmission electron  
845 microscopy images of native (left) and UHT heat-treated casein micelles (right).

846 **Fig. 3.** Atomic force microscopy (AFM) imaging and force spectroscopy experiments  
847 performed to measure the adhesion between milk proteins and milk fat globules (MFG)  
848 isolated from milks that have been either homogenized (H-MFG; left) or heat treated at ultra-  
849 high temperature and homogenized (UHT-H-MFG; right). (A) AFM topography images of  
850 MFG immobilized on filter membranes. (B & D) Adhesion force maps recorded at pH 6.7 and  
851 4.5, using AFM probes modified with native- (left) or with UHT-casein micelles (right). The  
852 percentages are the rates of force curves with specific adhesion. (C & E) Examples of  
853 retraction force curves obtained from each force map recorded at pH 6.7 and 4.5. All  
854 experiments were performed at 22°C in PIPES buffer.

855 **Fig. 4.** Parameters extracted from retraction curves recorded by atomic force microscopy  
856 (AFM) force spectroscopy to examine the adhesion between casein micelles and milk fat  
857 globules (MFG) isolated from milks that have been either homogenized (H-MFG) or heat  
858 treated at ultra-high temperature and homogenized (UHT-H-MFG). Boxplots showing the  
859 distribution of (A) the maximal adhesion forces  $F_{adh}$ , and (B) the maximal rupture distance

860  $D_{adh}$ , measured at pH 6.7 and 4.5. The number of analyzed individuals (n) is shown for each  
861 set of experiments. The bold lines in the boxes indicate the median values. (\*\*\*) indicates  
862 significant differences, with  $P < 0.001$ , using the Wilcoxon test.

863 **Fig. 5.** Microstructure of milks and acid gels observed by confocal laser scanning microscopy  
864 (CLSM). CLSM images of milks at pH 6.5: (left) milk homogenized at 20 MPa; (right) milk  
865 heat-treated at ultra-high temperature (UHT: 140°C, 4 sec) and homogenized at 20 MPa.  
866 CLSM images of the acid gels obtained at pH 4.5. In the CLSM images, proteins are in green  
867 while the triacylglycerol core of fat globules is in red. Scale bars are 5  $\mu\text{m}$ . Arrows indicate  
868 stranded structures in the acid gel formed from UHT heat-treated and homogenized milk.

869 **Fig. 6.** Evolution of the storage modulus  $G'$  as a function of the decrease in pH measured for  
870 homogenized milk (H-milk; blue) or milk that has been heat treated at ultra-high temperature  
871 and homogenized (UHT-H-milk; red). Analysis of variance: \*\*\* indicate significant  
872 differences with  $P < 0.001$ .

873

874 **Fig. 7.** Schematic representation, from nanoscale inter-particle forces to bulk properties, of  
875 the interactions between casein micelles and milk fat globules (MFG) in non-heated  
876 homogenized milk or ultra-high temperature (UHT) heat-treated and homogenized milk, with  
877 the consequences on the microstructure and rheological properties of the respective milk acid  
878 gels formed at pH 4.5. The green arrows represent the adhesion forces between homogenized  
879 MFG and casein micelles as determined by atomic force microscopy. CLSM images show the  
880 proteins (in green) and the MFG (in red) in the network formed at pH 4.5.

881

882

883

884

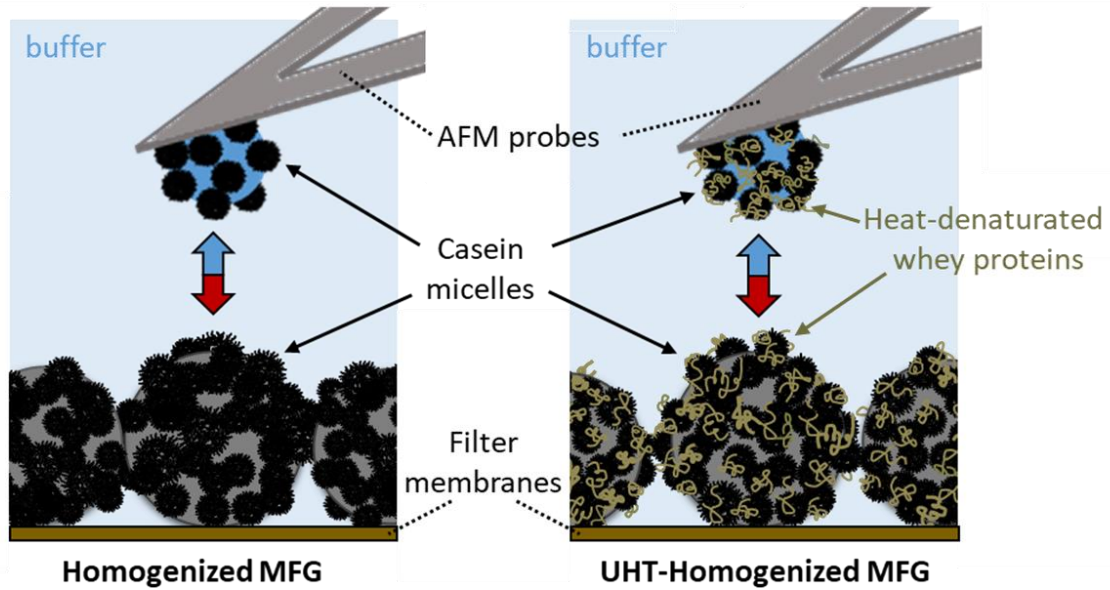
885 **FIGURES**

886

887 **Figure 1**

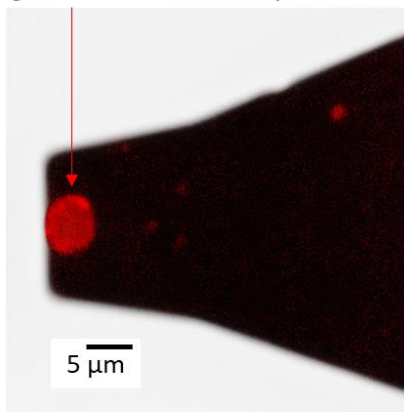
888

**(A) AFM force spectroscopy**

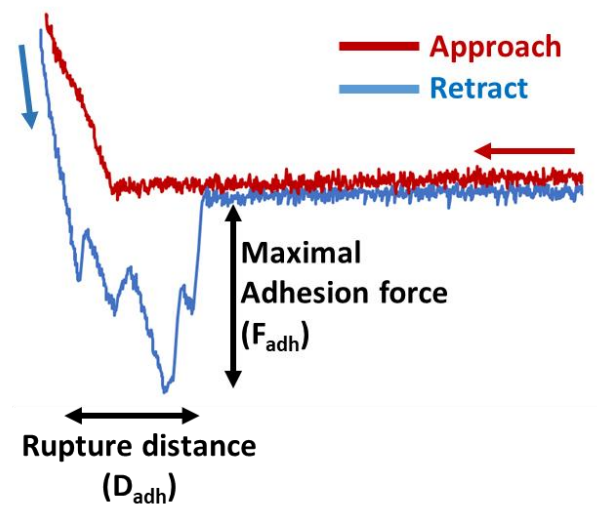


**(B) AFM probe**

Fluorescently-labelled caseins grafted on the AFM probe



**(C) AFM force curve**



889

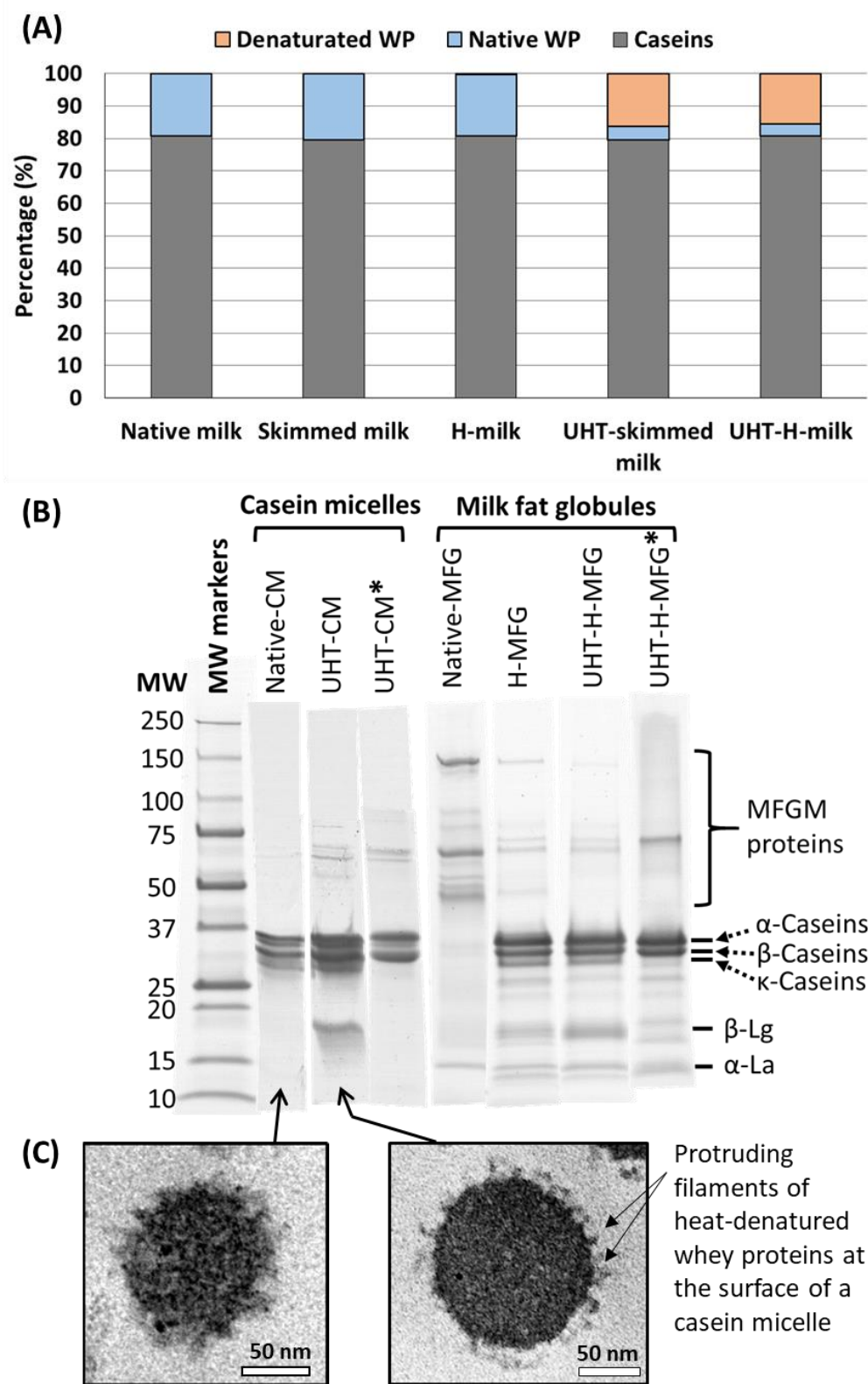
890

891

892

893 **Figure 2**

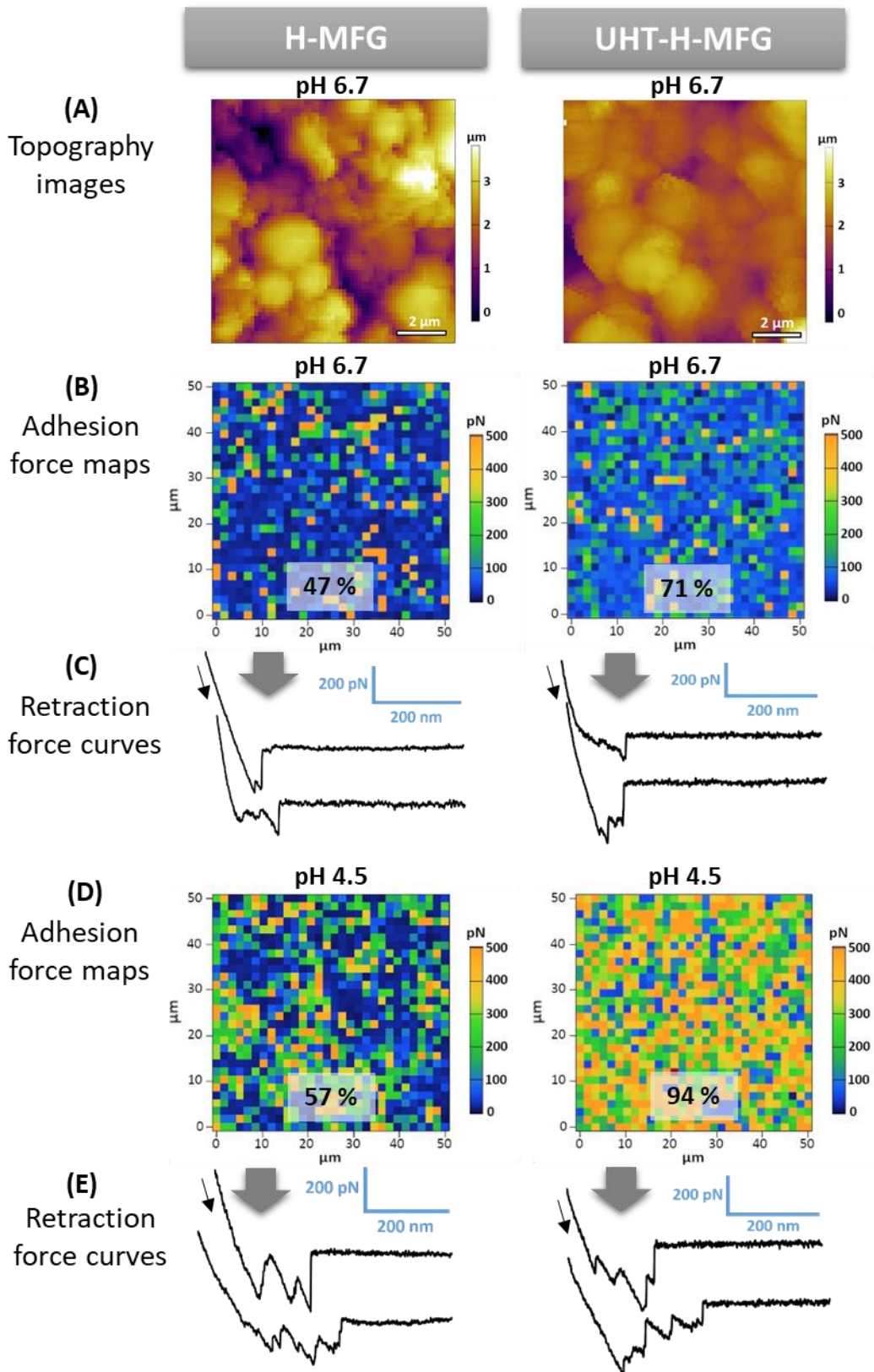
894



895

896

897 **Figure 3**



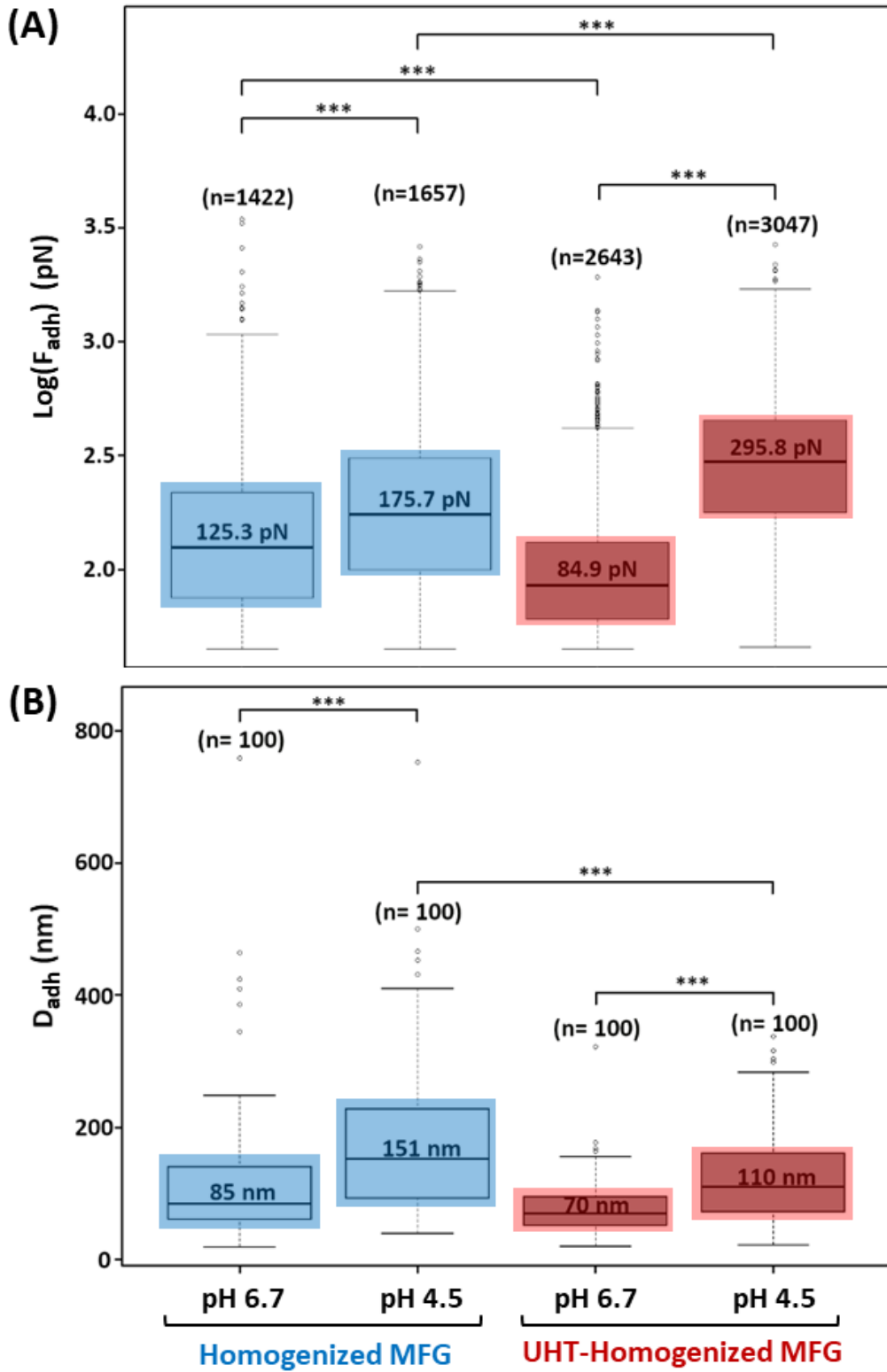
898

899

900



901 **Figure 4**

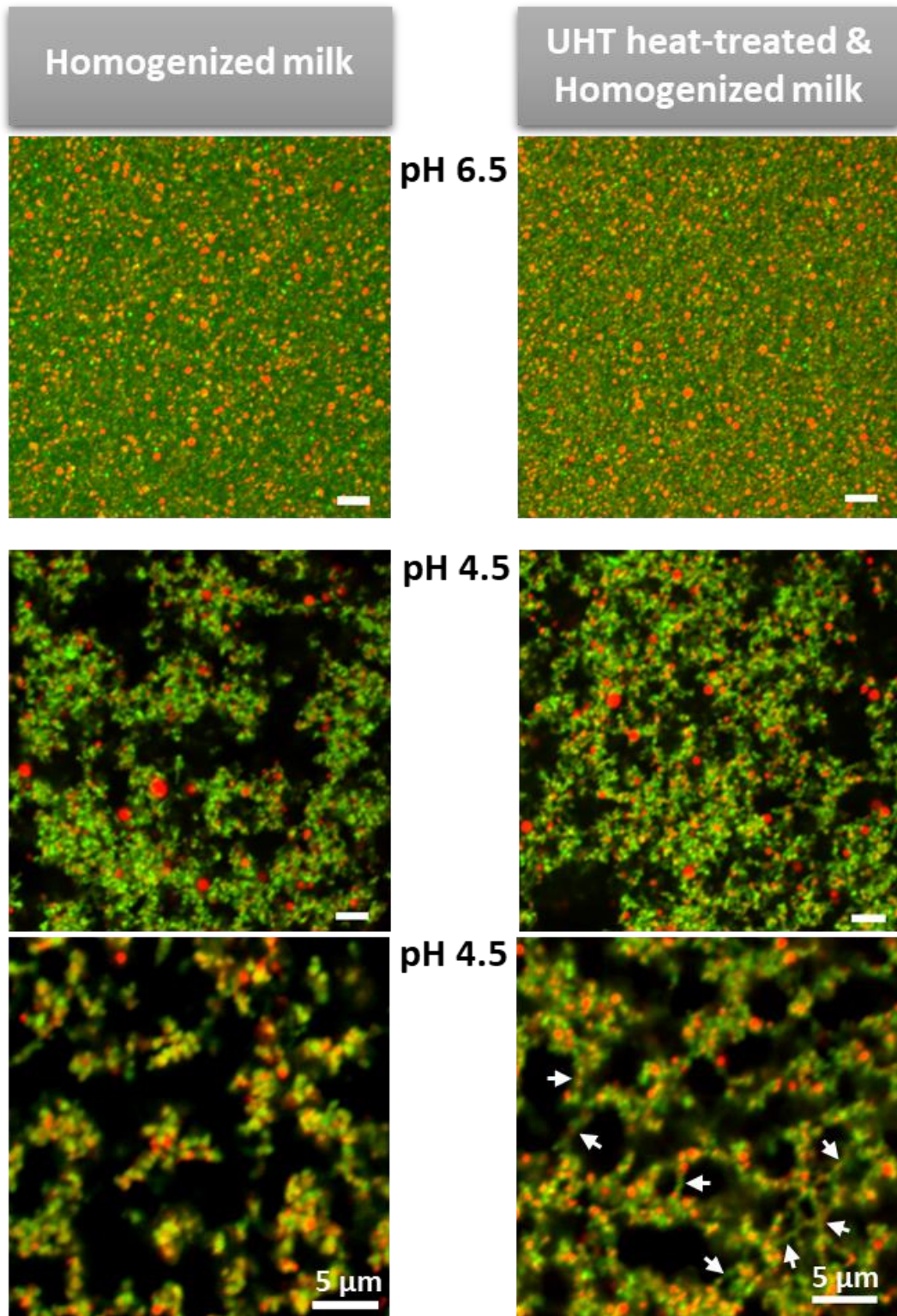


902

903

904

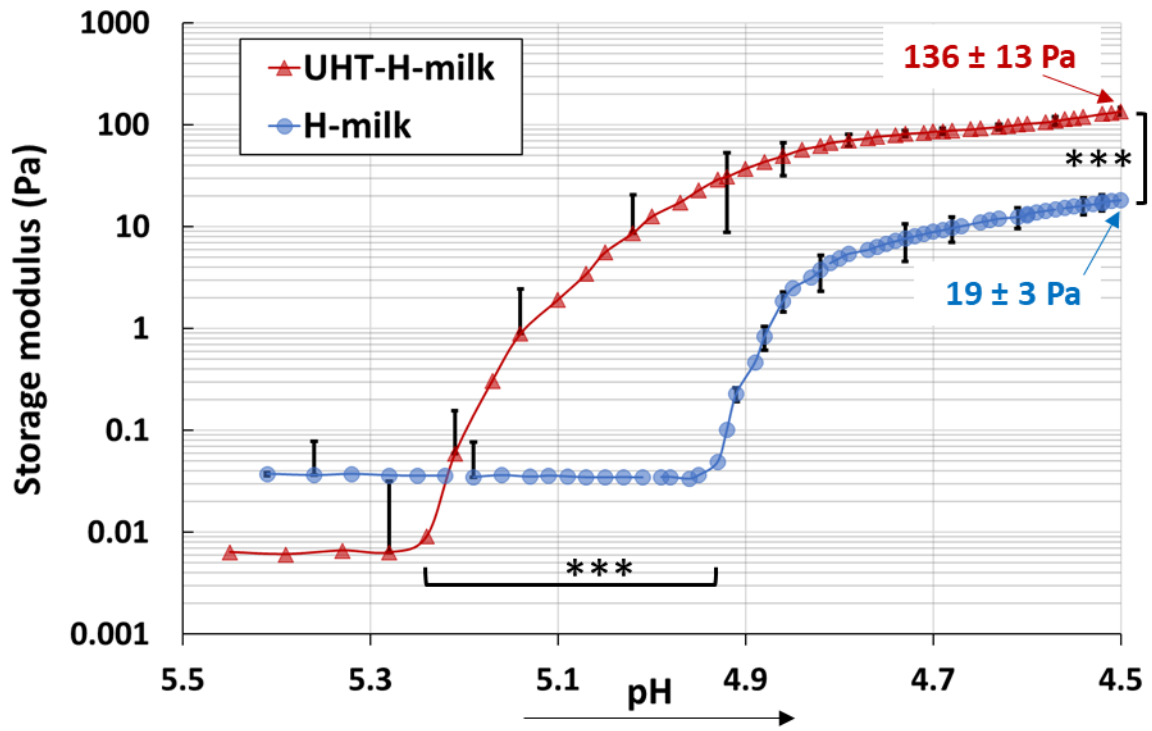
905 **Figure 5**



906

907

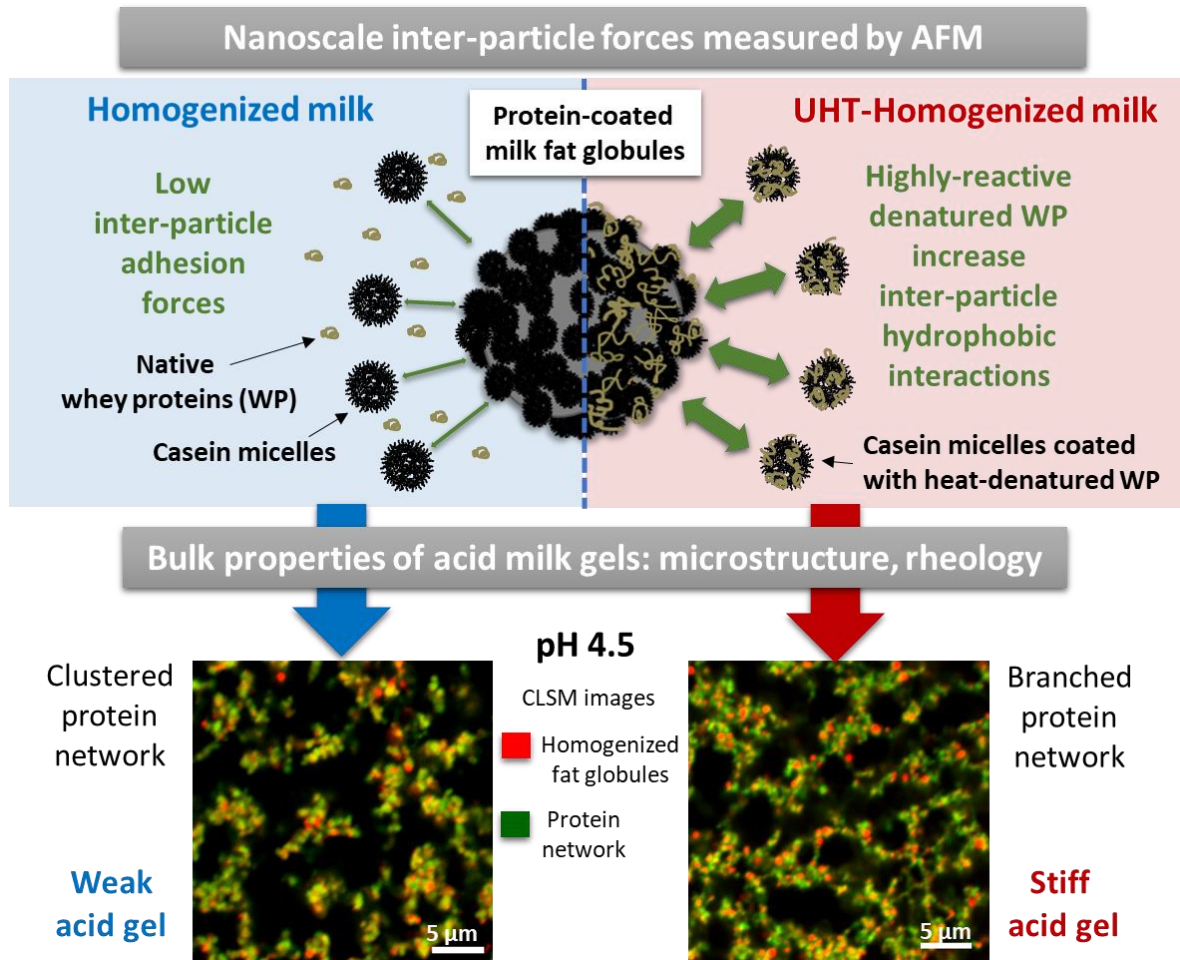
908 **Figure 6**



909  
910  
911  
912  
913  
914

915 **Figure 7**

916



917

918

919

# WHAT'S IT LIKE OUT THERE? LANDSCAPE LEARNING DURING THE EARLY PEOPLING OF THE HIGHLANDS OF THE SOUTH-CENTRAL ATACAMA DESERT

Rodrigo Loyola<sup>1</sup>  
Lautaro Núñez<sup>2</sup>  
Isabel Cartajena<sup>3</sup>

<sup>1</sup>UMR 7055 Prehistoire et Technologie (PreTéch), Université Paris Ouest Nanterre La Défense, 92023, Nanterre Cedex, France. E-mail: rodarkeo@gmail.com

<sup>2</sup>Instituto de Arqueología y Antropología (Instituto de Arqueología, Antropología y Museo), San Pedro de Atacama, Universidad Católica del Norte, Gustavo Le Paige 380, San Pedro de Atacama, Chile. E-mail: lautaro.nunez@hotmail.com

<sup>3</sup>Departamento de Antropología, Universidad de Chile. Ignacio Carrera Pinto 1045, Ñuñoa, Santiago, Chile. E-mail: isabel.cartajena@gmail.com

## Abstract

It has often been assumed that a link exists between climate change and human dispersion during the initial peopling of the Atacama Desert. However, there is little understanding of how hunter-gatherers acquired and processed environmental information. We examine paleoenvironmental and archaeological data to propose that the early peopling of the highlands of the south-central Atacama was a gradual process modulated by landscape learning. Evidence suggests that initial occupations at the end of the Pleistocene were limited to intermediate altitude levels, where the ecological structure was more easily legible and productive. This allowed human groups to make use of general, transferrable landscape knowledge, based mainly on the hunting of wild camelids and the gathering of plant resources in azonal formations. However, the arid event of the Early Holocene led to successive episodes of abandonment and relocation to new areas, consolidating complementary land-use between the desert lowlands and the high puna. Two complementary strategies for the acquisition and transmission of information can be identified: (1) scouting as part of logistical hunting parties; and (2) information-pooling rooted in broad, flexible social networks. We conclude that in the face of uncertain conditions, hunter-gatherers invested more effort in learning the landscape and sharing environmental knowledge.

**Keywords:** Landscape learning, Highlands, Atacama Desert, Early peopling.

## 1. Introduction

The initial peopling of the highlands of the south-central Atacama (21-24°S) is related to the "Tuina-Tambillo" phase (13,000 to 9500 cal BP). From early in this period, small hunter-gatherer bands developed a lifestyle well adapted to high-altitude deserts of the Salt Puna eco-region (Fig. 1). The development of a generalist technology, broad-spectrum subsistence and a seasonal mobility pattern enabled them to complement the wide variety of resources available in the different altitude levels of the Andes range (Núñez and Santoro, 1989; Núñez et al., 2002). Most authors agree that the Pleistocene-Holocene humidity peak played an important role in early human dispersal by offering more productive habitats. However, the spatial and temporal discontinuity of the archaeological record suggest a much more complex scenario. While some patches show occupation from an early date, others were abandoned, or only occupied later, while some areas were avoided completely. Clearly, it is not possible to establish a direct link between human dynamics and resource availability. Instead, a focus on "how" hunter-gatherers acquired and transmitted environmental knowledge could be an appropriate way to evaluate the rate of human dispersal and habitat preferences.

Many questions remain unanswered, but three are of particular interest for our case study: What prior knowledge existed? What had to be learned and what barriers did human groups face? What strategies were used to acquire landscape information? Landscape learning is a suitable approach for addressing these questions (Rockman, 2003, 2009), but not particularly easy to infer from the archaeological record (Kelly 2003). Mainly, because the acquisition and transmission of knowledge occur primarily in the social arena (Tolan-Smith, 2003). We will therefore examine the temporal and spatial variability of the archaeological record from a multi-

scale approach. The study of lithic technology provides an important line of evidence, as it allows us to explore the behavioural and cognitive dimension behind human dynamics in the landscape. We will show that populations dispersed progressively and selectively as this “Mars-like” landscape was learned. Complementary strategies to acquire and transmit information counteracted the partial uncertainty during human dispersal, as well as the negative climate fluctuations of the Early Holocene. In the long term, the new knowledge fostered deep changes in social organization, leading to a growing specialization in the high-altitude desert environment.

## **2. Landscape learning and environmental knowledge**

Landscape learning is a staged process in which human groups acquire, transmit and store knowledge about the environment that they inhabit (Meltzer, 2003; Rockman, 2003, 2009). It encompasses a series of interrelated sub-processes occurring on different temporal and spatial scales, ranging from individual experience, through the intergenerational time of a local group, to adaptive radiations in human evolution. Although more emphasis has been placed on exploration and initial colonization, for hunter-gatherers learning the landscape is a critical and constant activity (Milne, 2014). In an immediate-return economy, even small disturbances in the climate and resource structure could have serious effects that must be anticipated and predicted. Besides, environmental cognition is a complex task mediated by mental models that are constantly evolving and being updated (Golledge, 2003), thus it is always imprecise and never completed (Meltzer, 2003). Foragers must therefore spend a large part of the time in acquiring and rectifying information during their daily social interactions (Fitzhugh et al., 2011). Landscape learning is thus a day-to-day task occurring in the social arena (Tolan-Smith, 2003), in which two aspects are vital: mobility and social networks. While the former takes individuals to places to observe, the second is the architecture through which information flows.

When a new territory is populated, the incoming population does not start from zero (Meltzer, 2003). If there are no other resident groups or even their traces to extract information, the knowledge acquired in their previous habitats can be good basis for generating expectations (Steele and Rockman, 2003), and often promotes exaptive advantages (Gamble, 1993). However, applying preconceived environmental models without taking into account the specific configuration of the new landscape can lead to false predictions, sometimes with catastrophic results. Human groups have to reach a balance between the unknown consequences of using their prior knowledge and the investment of critical time to acquire new learning (Meltzer, 2003). For this reason, populations prefer “legible” landscapes (Golledge, 2003), in which processing demands are low and generalised knowledge can be successfully applied. Environmental homogeneity is an important factor in this context (Gamble, 1994): more continuous, rapid dispersal can be expected in macro-environmental zones with a similar set of resources (Beaton, 1991; see also Osorio et al., 2017). Initial populations are better prepared to track “gross habitats” (Meltzer, 2004) which become more spatially specific and differentiated only with increased residence time, even if this inhibits the ability to continue dispersing (Wren and Costopoulos, 2015).

At least three components of the landscape have to be learnt: regimes, routes and resources (Meltzer, 2003). Track regimes require users to recognize and predict a broad variety of climate patterns such as temperature oscillation, precipitation, annual snowfall, etc. Knowledge of regimes normally extends from the specific to the general. Since climate is experienced over a few years within the life of an individual, intra-annual variation and even some decadal fluctuations can be learned easily, unlike those occurring in centennial-millennial cycles (Meltzer, 2003). Learning and tracing routes involves a different cognitive process known as wayfinding in which individuals identify and interpret parameters of the landscape as they move through it, using memory and the spatial knowledge base to go from one place to another (Golledge, 2003). In complex environments, more time is invested in the creation of rigorous cognitive maps in order to avoid the risk of getting lost (Golledge, 1999). Initially, settlement systems would consist of a few stable points (landmarks) using prominent topographic and geographic features as references and connected by safe pathways such as natural corridors. Over time, they evolve into more complex layout-based systems with a greater number of landmarks and links (organized according to their frequency and purpose of use) in which nested areas are differentiated around them (Golledge 2003). In this case, the associated

knowledge goes from the general (or "extensive") to the specific. Learning about resources depends on their reliability, availability and predictability (Rockman, 2003). In the case of fixed, permanent resources, such as sources of lithic raw materials or water, knowledge is less transferrable since it depends on local factors. Impermanent resources on the other hand, require the development of limitational knowledge about their characteristics, boundaries and costs (Rockman, 2009). However, it can be transferred over larger regions, especially in the case of bigger, more mobile animals (Kelly and Todd, 1988; Gamble, 1995; Kelly, 1995).

## 2.1 Scouting, hunters and trackers

Hunter-gatherer societies use different strategies for learning the landscape. Scouting is a common activity for acquiring information through direct observation during rapid exploratory forays (Meltzer, 2004). However, exploring is rarely the sole objective of these expeditions and scouting is usually embedded in hunting parties (Roebroeks, 2003). Tracking and stalking animals, or simply following their trails allows routes and wildlife ranges to be mapped and new patches of resources incorporated into cognitive maps (Nieves and Stoffle, 2003). Hunting is a complex cognitive task in itself, that entails high information-processing requirements and real-time resolution of spatial problems in a coordinated and collective way (Tolan-Smith, 2003). During their forays, hunters depend primarily on a route-based knowledge and several wayfinding strategies such as "piloting" (navigate between distant landmarks) and homing via "path integration" (dead reckoning) (Golledge, 2000). For this reason, scouting trips are commonly conducted by expert hunters and trackers with advanced wayfinding skills, motivated not only by the acquisition of resources but also by the chance to gain social prestige (Fiedel and Anthony, 2003).

In a state of partial uncertainty, scouting provides additional information to support the decision-making on what to do next (Jochim, 1976). Large-scale migration generally involves a previous scouting phase (Hegmon and Fisher, 1991), however scouting can also be a constant activity during the annual cycle to incorporate fall-back or full-use areas (Nieves and Stoffle, 2003), or when game is scarce (Binford, 2001:454). Information about a large area or from focused events can be captured quickly and at low cost, however, its circulation is restricted to the local or inter-band network (Fitzhugh et al., 2011). These expeditions are composed of one or a few individuals who quickly move out of their home range in search of prey. Logistical mobility is probably the best option since it imposes fewer limitations on movement and greater risks can be taken (Kelly, 2003). Scouting trips can cover long distances and in some cases last for several months (Binford, 2001). During the course of the expedition, short-term specialized task camps are used for one or a few nights, principally for overnight stays, fire maintenance, tool replacement and repair, processing of captured prey animals and discrete consumption (Lovis, 2005). Within their cognitive maps, scouts and hunters can manage a wide repertoire of potential refuges in case of need, such as caves and shelters (Walthall, 1998).

## 2.2. Information pooling and hunter-gatherers' networks

During their face-to-face interactions, individuals establish and strengthen bonds with other individuals and so expand their personal networks; in this way, knowledge of the landscape available beyond their local niche can be transmitted and updated. Foragers invest time and resources in networking, often for the purpose of acquiring relevant information of the environment – even of distant, unknown areas beyond their direct experience (Silberbauer, 1981). Regular, multi-band aggregations for periodic ceremonies, trading fairs, collective tasks, etc. are good opportunities for members of neighbouring groups to update and exchange knowledge (Fitzhugh et al., 2011). They allow information to be acquired in large volumes and at a low cost by indirect or "down-the-line" transmission. However, as the distance increases, the information is more prone to distortion, and accurate information of remote areas is more selective as well as costlier; it requires the investment of a greater amount of energy and material resources in order to maintain stable, frequent interactions (Fitzhugh et al., 2011). In this context also, logistical mobility is an important strategy for supporting visits between reciprocal partners, trade expeditions, pilgrimages or extended journeys. Given the greater distances, these interactions generally involve the exchange gift-giving of non-utilitarian goods in order to ensure the strength of social ties (Whallon, 2006).

In forager societies, mechanisms for circulating information are mainly verbal and co-presential and this implies a greater risk of loss or distortion. In the absence of material supports, the only way of storing knowledge is in individual memory (Whallon, 2011). Maintaining large, cohesive networks allows the environmental information acquired through direct observation (after scouting, for example) and individual experience to be pooled and transferred to larger social units (Tolan-Smith, 2003). In this way, knowledge of the landscape can be transmitted not only in space, but also in time through intergenerational exchange, allowing events of greater amplitude to be tracked, with an interannual-decadal or even centennial frequency (Fitzhugh et al., 2011).

### 3. Regional Settings

#### 3.1. The current landscape

The structure of the highlands of the south-central Atacama (Fig. 2) is modelled by two major morphostructural units: the Domeyko precordillera to the west, and the Andes Mountains, rising to above 6000 masl, in the east (Fig. 3A). This abrupt vertical gradient determines a strong contrast in precipitation regimes: while the mean annual precipitation (MAP) is close to 300 mm at 5000 masl, below 2300 masl it can decline rapidly to less than 1 mm (Houston, 2006a). Currently, more than 85% of the annual rainfall occurs during the southern summer (December to March), when moist air masses are transported from the Amazon, triggering intermittent convection storms (Garreaud et al., 2003). In contrast, winter rainfall is related to the Pacific moisture which penetrates from south-central Chile, often in the form of snowstorms (Vuille and Ammann, 1997). On an inter-annual time-scale, rainfall regimes are modulated by El Niño Southern Oscillation (ENSO) (Houston, 2006b). During La Niña, summer rainfall tends to increase producing massive flooding; conversely, extreme winter precipitation and summer droughts are associated with El Niño phase. While precipitation regimes can present significant irregularity and unpredictability (Romero et al., 2013), groundwater recharge represents a more reliable fresh water source (Houston et al., 2016b). The saline lakes and salt flats located on basin floors are fed by numerous inflows which discharge their water into the hydrological base in the form of diffuse seepages, flowing springs, perennial rivers and aquifers (Risacher et al., 2003).

Compared with the northern Atacama, the flora becomes poorer further south due to the greater aridity. At this latitude (21-22°S), the maximum inland penetration of the desert reaches 2700 masl (Arroyo et al., 1988), above which an herbaceous and shrubby zonal vegetation develops, distributed in altitude-conditioned vegetation belts. At least four such belts can be recognized in the study area (Fig. 3B): (1) pre-puna (2700-3100 masl), characterized by semi-desert deciduous shrubs, succulents and cacti; (2) puna (3100-3750/3900 masl), scrub dominated by shrubs or *tolas*; (3) high puna (3750/3900-4400 masl), composed of shrubby steppe (caespitose perennial grasses or “pajonal”); and (4) the subniveal belt (>4400 masl) which marks the upper limit of the vegetation (Aldunate et al., 1981; Villagrán et al., 1981, 1998).

In contrast, the azonal vegetation maintains permanent cover throughout the year. Currently, some 264 active wetlands, marshes and bogs have been identified in the region (DGA, 2004). They are dominated mostly by species of reeds, grasses and cushion plants, which grow round the margins of lakes and salt flats and on the banks of canyons (Villagrán and Castro, 1997). Even in the arid lowland desert, azonal vegetation grows in scattered oases, supporting low-elevation wetlands and trees such as tamarugos (*Prosopis tamarugo*), algarrobos (*Prosopis alba*) and chañar (*Geoffroea decorticans*) (Villagrán et al., 1998). Azonal formations are vital for fauna. The majority of animals are residents and reproduce in the region, especially less mobile species; these include micro mammals such as chinchilla (*Chinchilla brevicaudata*) and vizcacha (*Lagidium viscacia*). Larger species such as wild camelids (*Vicugna vicugna* and *Lama guanicoe*), canids (*Lycalopex culpaeus* and *Pseudalopex griseus*) and felines (*Lynx chaus* and *Lynx baileyi*) can travel great distances and reproduce outside the area.

#### 3.2. Paleoenvironment and climatic changes



The Atacama is one of the oldest and driest deserts on earth, however the paleoenvironmental record shows a dynamic past marked by pulses of higher humidity. After the Last Glacier Maximum (LGM), a climate change event known as the Central Atacama Pluvial Event (CAPE) increased summer precipitations in the Andes region in two phases (Latorre et al., 2006; Quade et al., 2008; Placzek et al., 2009). The first is known as CAPE I (17.5-14.2 ka BP) and affected mainly the Central Andes; in contrast, CAPE II (13.8-9.7 ka BP) was much more intense and prolonged in the south-central Atacama. During this phase, the rainfall was 3 to 5 times higher than today, reaching a mean annual precipitation of 400-500 mm (Grosjean et al., 2001). Some lakes of the high puna grew to more than six times their present area. Water bodies covered nearly 8% of the area as opposed to barely 0.9% as now (Kull and Grosjean, 1998). Particularly illustrative have been the studies in Miscanti (4140 masl) (Fig. 4A) which show higher lacustrine levels between 14 and 9.5 ka BP, disrupted by a short arid interval around 11.6 ka BP (Grosjean et al., 2001).

The higher hydrological recharge also raised the levels of subterranean water tables in pre-Andean basins, forming large wetlands, marshes and bogs (Rech et al., 2002; Quade et al., 2008; Sáez et al., 2016) (Fig. 4B, Fig. 4C). As result, the diversity and abundance of plant species increased considerably. Steppe grasses currently relegated to the high puna descended, while northern plant species extended at least 50 km south of their modern ranges (Betancourt et al., 2000; Latorre et al., 2002, 2003; Maldonado et al., 2005). Some studies indicate that the primary productivity was 10 to 20 times greater than at present, allowing the development of 50 to 80% plant cover, compared to <5% now (Latorre et al., 2002) (Fig. 4D). Even on the desert floor, peats and organic paleosols with gastropods and layers of diatomites have been dated to around 11.2-10.5 ka BP (2200 masl), showing that the lacustrine environment and marshes of the Atacama salt-flat expanded 1200 metres beyond its current border (Núñez et al., 2005). Similar evidence has been found in saline cores extracted from the Atacama salt flat, revealing an Early Holocene wet phase from 11.4 to 10.2 Ka (Bobst et al., 2001). Humid conditions extended even into the Central Valley, as recently indicated by the analysis of organic and saline sediments in Pampa del Tamarugal (900-1000 masl) (Nester et al., 2007; Gayó et al., 2012) and the lowlands of the Antofagasta region (900-1600 masl) (Pfeiffer et al., 2018).

However, during the second part of the Early Holocene, the aridity increased drastically in the South-Central Atacama (Sáez et al., 2016), and this situation became more severe during the Middle Holocene (Grosjean et al., 2001, 2003). Although the impact of this climate change on human dispersal is still unknown, it triggered a drastic reconfiguration of hydric and biotic resources. Some areas were more severely affected than others. In the high puna, the lakes contracted and most of them dried out (Messerli et al., 1993; Grosjean et al., 2001), while wetlands on the pre-Andean floor collapsed permanently (Latorre et al., 2003; Grosjean et al., 2005; Quade et al., 2008).

#### **4. Sites and stratigraphic contexts**

The archaeological sites studied in this work (Fig. 5) are located in the highlands (2000-4500 masl) of the south-central Atacama (21-25°S), covering a temporal range spanning from 13,000 to 9000 cal. BP (Table 1). In the case of the sites in caves and rock shelters, no important disturbance problems are recorded (Núñez et al., 2005). Conversely, differential vertical selection processes have occurred in the open-air sites; this means that archaeological remains have been redistributed in the vertical axis according to their size, shape and weight, generating a mainly superficial record with low stratigraphic potential.

#### **5. Climate regimes**

Climate regimes are among the most important component of the environment that must be learned in arid landscapes, since meteorology controls the availability and timing of water recharge. The spatial distribution of the sites and the radiocarbon dates obtained provide a first approach to this problem. As Figure 6 shows, during the Late Pleistocene there was continuous occupation from 13,000-11,000 cal BP, restricted to the pre-puna belt (2600-3200 masl) where no temporal gaps are observed (Fig. 6). The wetlands, bogs and marshes formed during CAPE

It offered productive habitats in the pre-puna floor between the high puna and the lowland desert, which were subject to less seasonality and minor resource incongruence. Given the longitudinal climate gradient, the spatial distribution of the sites would have allowed to access to a wide variety of complementary environments on the same altitude floor.

Intra-annual variability must certainly have been learned quickly, as well as those interannual-decadal events which can be experienced within a lifetime. On the other hand, periodic events occurring on a centennial scale and longer-term changes were more difficult to predict and anticipate. This may be the case of the prolonged drought episodes that caused the abrupt fall in lake levels in Miscanti Lake around 11,600 cal BP (Grosjean et al., 2001), and the oxidized horizons and eroded surfaces in SPN-1 (Grosjean et al., 2005). Although this arid event has not been explored in depth, it occurs contemporaneously to a notable gap in the archaeological signal around 11,500 cal BP. Only after 10,700 cal BP, some sites are reoccupied while others seem to have been re-sited close to more stable water resources – like SPN-19/20 located in the alluvial fan of the Frio River (Cartajena et al., 2014), and TU-109/E-IV placed in the upper course of the Tulán River. In situations where the group is unable to predict the length, amplitude and periodicity of climate changes, temporary abandonment of some sites and territorial change could be a good strategy to evade resource failure and water scarcity. It is precisely during the archaeological gap that incursions into low-elevation wetland areas of the desert level are observed in Tam-2/4a and TU-68 (Núñez et al., 2005).

As the arid conditions of the second part of the Early Holocene settled, the pre-puna was definitively abandoned about 9700 cal BP after the paleo-wetlands dried up and became phreatic beaches. Almost simultaneously, the previous occupations of the desert lowlands gave way to the large multi-seasonal camps at TA-1, and others on a smaller scale such as at TU-67. Stable access to the high puna is noticed in sites such as AC-1, TUY-1, and SM-4, and several other sites that to date have not been dated. Even today, occupation of this area is restricted to summer when the snow melts and grasses are more productive because of the summer rains. It could be argued that greater knowledge of intra-annual variability allowed groups to deploy a settlement/mobility system based on semi-permanent settlement of the lowlands combined with seasonal access to the high puna. This would allow efficient exploitation of resources according to their seasonal availability in the landscape. In the long term, greater systemic resilience was achieved and groups coped better with climate fluctuations and unpredictable events.

## **6. Routes and pathways networks**

Learning routes means internalizing at least two aspects: the location of places and the structure of the paths that connect them. Sites can be divided into two main location patterns (Fig. 7). One group consists of open-air sites placed on fluvial terraces and phreatic beaches around the borders of salt-flats and saline lakes (Table 2); their record consists mainly of surface scatters on modern sedimentary units (Qa, PPI1c), and aeolic litho-stratigraphic units (Qe) related with alluvial activity dating from the Pleistocene-Holocene (Fig. 8). The advantage of open-air camps is that they can be sited directly in the area where resources are available, supporting a practically unlimited number of people; however, this requires the repeated manufacture of stone structures, or use of tents, which have to be dismantled, transported and set up again in every residential move. The second group consists of sites located in rock-shelters and caves on the sides of ravines in the western Andes and the precordillera range (Table 2). Locations of this type are available mostly in volcanic outcrops or under ignimbrite beds exposed by lateral erosion in the walls of ravines (Fig. 8). While caves and rockshelters offer protected environments that require less work investment, their use is severely limited by their availability in the landscape, which may mean less than optimal location with respect to resources, and the often small size of their interior space. By making use of a combination of rockshelters and open-air sites, a balanced relation between mobility costs and distance to resources can be achieved.

Pathway networks (the material expression of routes) are harder to study, mainly because they are not conserved in the archaeological record. However, by using least-cost path analysis we can at least estimate the potential routes that impose the fewest limitations on human displacement. This is not a minor issue in a steep relief like that of the Andes, where slope and elevation are critical factors for mobility. During the Late Pleistocene, the distribution of

settlements not only enabled access to a wide diversity of environments, but great altitudinal contrasts were avoided by maintaining sites within a single ecological floor. Furthermore, the pre-puna facilitated wayfinding thanks to the presence of prominent topographical markers in the Andes and Domeyko ranges, which run parallel in a north-south direction. The preandean basins formed between the two ranges constituted a natural corridor at intermediate altitudes, where the effects of hypoxia are still slight. Certainly, the bottoms of the basins and borders of salt flats were the lowest-cost, safest routes. On the other hand, walking times between the sites not to exceed one day's march (8hrs) (Fig. 7). Such itineraries would have allowed the deployment of short-term pathways used during everyday activities whose accessibility would not have been seriously affected by seasonal or climatic factors. This does not mean that the sites were synchronous, but it allows us to estimate the distances between different relatively contemporaneous localities.

During the Early Holocene, a vertical mobility pattern connected the lowlands and the high puna along an east-west axis of about 70 km, with a drastic altitude range from 2000 to 4500 masl. Of course, this posed new and contrasting challenges to route-learning: on the one hand, the flat, featureless relief of the arid desert lowlands made wayfinding more difficult and riskier; on the other, the steep landscape and hypoxia considerably limited displacement within the high puna. Above 3800 masl, decisions on when and where go up there are critical since even today adverse weather conditions impede access for most of the year. Ravines and canyons seem to have been the safest, optimal routes, and not only for the lower slopes; their rocky walls and caves could be used as refuges or as outposts to monitor the weather, waiting for the right moment (De Souza, 2004:39).

Cognitive maps included a large number of landmarks and links between them, and areas which were organized according to their seasonal availability throughout the annual-round. Moving in such a complex layout system surely required a deeper route-based knowledge, the more so in a changing environment. The large number of Early Archaic sites in the high puna could be the result of successive adjustments in settlement location as lakes dried out (Fig. 7). For instance, SM-4 is both the latest site chronologically and that located closest to the edge of the lake at its current level (Núñez et al., 2002); the same is true of the large number of sites in the Tambillo oasis. Since the camps were mainly open-air sites, greater flexibility is apparent in their placement selection. In this scenario, paths and routes were more hierarchically organized. Some were used daily within an ecological floor, others were used seasonally during the displacement of the group between adjacent or distant ecological floors. Some must also have allowed travel to remote areas outside the region during intermittent journeys, requiring the group to cross challenging barriers such as the Andes Mountains and the arid plains of the central valley.

## **7. Resources**

### **7.1. Fresh water**

Fresh water is a fixed resource but its availability can be strongly affected throughout the annual cycle. Furthermore, water quality and composition can vary widely, even between sources located a few metres away from one another. Most have a high salinity (according to the amount of Total Dissolved Solids, Fig. 8) or a high content of elements such as arsenic and boron (Risacher et al., 1998). Not only must the location of waterholes be learnt but also their characteristics and limitations for human consumption. Not surprisingly, almost all the sites are located near the few good quality water sources. These are mainly flowing springs, probably because rivers and lakes have high salinity due to the evaporation rate.

While Late Pleistocene sites are generally located in currently dry environments, there are active springs within a few kilometres (i.e. Fig. 8A and B). In the case of Imilac and Punta Negra basin, sites are placed at the border of salt-flats close to high quality groundwater sources. However, the modern water table is at a depth of 70 meters (Risacher et al., 1998) and therefore inaccessible (Fig. 8C, 8D, 8E and 8F). It can be established that Late Pleistocene settlements were occupied only when groundwater levels were high; once the fresh water sources dried up or became inaccessible, the sites were abandoned. Conversely, Early

Holocene sites, especially from the second part of the period, are located directly at currently active water sources. This may be due to two reasons: the greater water availability stress to which the settlements were subject and the reconfiguration of hydrological cycles as aridity increased. The high puna sites are located directly at good quality springs exposed when the lakes contracted to their current size (Fig. 8 G.H and I), while the occupation of the lowlands coincides with the formation of groundwaters in the Atacama salt-flat (Fritz et al., 1979) (Fig. 8J and 8K).

## 7.2. Rocks

Knowledge of lithic resources is less transferrable since it depends on local factors such as geology and geomorphology. The resources which were easiest to identify in the landscape were quickly acquired once their location became known (Ford, 2011). Coarse-grained rocks such as basalts, andesites and felsites can be found in large, highly-visible primary formations related to mountainous geofoms, which also explains their high frequency in assemblages (Fig. 9). Such is the case of the extensive outcrops of tuff in Tulán Cerros (Fig. 8K) and aphanitic basalt in Morro Punta Negra (Fig. 8F) (Loyola et al., 2017). Siliceous rocks show a greater frequency, even though they are not always available locally; moreover, they are more difficult to identify. In this case, some patterns in the lithic landscape could be used as “schemata” (Golledge, 2003). In the highlands, white siliceous rocks are usually found in smaller residual sources included in secondary sedimentary deposits. Something similar occurs with chalcedonic breccias, which have been recorded in discrete hydrothermal craters on the northern edges of Imilac Salar (Fig. 8C). A few kilometres away, there was an extensive phreatic beach where small nodules of white flint of excellent quality have been found. An exception is the Talabre source, where several workshops has been documented associated with large outcrops of siliceous rocks (De Souza, 2010).

In the Andes, obsidian is found in small domes and lava-domes associated with large calderas and stratovolcanoes (Yacobaccio et al., 2004). A large number of the obsidians in the assemblages come from the local source of Pelún, north of the Salar de Atacama (Seleenfreund et al., 2010), demonstrating early knowledge of this source. Black obsidian, on the other hand, was acquired mostly from sources in the Zapaleri-Tara system located in the high puna, where it appears in the form of scattered small nodules (Fig. 8H); sites such as AC-1 ensured supply to lower floors, although procurement was seasonally restricted. Extra-regional obsidians are also recorded, sourced from sites in northwestern Argentina such as Tocomar and Quiron (Escola et al., 2016). Towards the Early Holocene, a substantial increase of transported obsidian is observed in the assemblages (Fig. 9), particularly extra-regional varieties. At the same time, some presumably local sources, such as grey obsidian which had not previously been exploited, achieve a wide spatial diffusion, suggesting deeper knowledge of the local lithic landscape.

## 7.3. Scanning plants

Although the lower biodiversity of plant species imposed a lower learning demand, the significant endemism of the native flora (Squeo et al., 1998) could disable the application of prior knowledge. The ecological floor structure defines specific altitude distributions for each species, whose growth habits, nutritional potential, limitations, functionality and availability throughout the annual cycle must be learnt. A general classification of the native flora, based on taxonomic and physiognomic similarities with already known plant species (of the same family, for example) could have been a good way to learn local plants (Villagrán et al., 1998). The case of azonal vegetation could be different. Due to the biogeographical expansion during the Late Pleistocene, azonal plant formations show a peculiar homogeneity throughout the Central and Desert Andes (Villagrán and Castro, 1997), constituting a more reliable and better-known source of plant resources. Unlike zonal vegetation, which follows seasonal growth timings, bogs and marshes maintain continuous, dense cover throughout the year, even during the cold season. Besides being the main source of forage for camelids, this formation is also the most important source of edible and medicinal plants, firewood, pigments, plant fibres and other resources such as eggs (Villagrán and Castro, 1997).

In the Late Pleistocene and Early Holocene sites, there is evidence of active paleowetlands, contemporaneous with human occupations, which disappeared with the increasing aridity. For instance, silt deposits have been recorded in Imilac and Punta Negra which contain epiphytic diatomites and Cyperaceae, as well as root marks, intercalated with peat layers (Grosjean et al., 2005), sponge spicules, algal testae and gastropods (Succineidae) (Quade et al., 2008). In the Tuina sites, steppe grasses, abundant summer annuals and tolar shrubs have been reported between 11,700 and 9600 cal BP (Latorre et al., 2003) (Fig. 8A). At the SL-1 site, the cultural material is contained in sand layers with abundant organic content and plant remains (Núñez et al., 2005) (Fig. 8B). Evidence of bulbs or succulent roots that grow during the rainy season was also recovered (Núñez et al., 2005).

Conversely, Early Holocene sites are directly associated with marshes and wetlands after the reconfiguration of water resources. In the case of high puna sites, there are bogs around the springs located at lake margins (Fig. 8G, H and I). The Tulán River sites are located a few hundred metres away from the Tchulin Marshes (Fig. 8K) (Betancourt et al., 2000; Latorre et al., 2002). In TA-1, plant macrofossils and gastropods dated to 11,190-10,580 cal. BP (Geyh et al., 1999; Núñez et al., 2005) have been collected from an area one kilometre to the east of the current shoreline, where there are now marshes and introduced Tamarugo forests (Fig. 8J). Arboreal resources seem to have acquired special importance at the end of the Holocene based on the appearance of profuse grinding technologies in TA-1 and chañar seeds recovered in TU-67(E-VII) (Núñez et al., 2002). The fruits of these trees grow during the summer, but if ground into flour they can be stored for a long time. It is difficult to specify whether these arboreal resources were known previously. In any case, learning how to process them would require some degree of observation and experimentation, which usually happens during periods of environmental change (Meltzer, 2003: 232).

#### 7.4. Animal-tracking

According to the available evidence, subsistence was based on a broad-spectrum generalist diet. The consumption of animals focused almost exclusively on modern fauna species with emphasis on wild camelids (*Vicugna vicugna* and *Lama guanicoe*), even when extinct mega fauna was available (Fig. 10) (Cartajena, 2003; Cartajena et al., 2006). Certainly, the tracking and capture of wild camelids required knowledge of their feeding behaviours, social organization, demography, seasonality, reproductive habits and migration routes. In an environment of high spatio-temporal incongruence of forage plants and heavy snowfalls, guanacos can develop seasonal migratory and reproductive patterns. It has been observed in several areas of the Andes that guanacos disperse into smaller units on lower floors during the winter, but as soon as the snow melts they return to the highlands for the summer breeding season (Franklin, 1982; Cartajena, 2003; Puig et al., 2011). Vicuñas on the other hand have more sedentary and territorial habits, limited to the upper floors.

Camelids can be found in most of the Andes Range, even in Patagonia in the case of the guanaco. They constituted one of the main resources in the diet of the early hunter-gatherer groups of the Andes, suggesting that their behaviour and ecological cycles were widely known. Unlike micro-fauna, larger, mobile game enables the use of more generalized knowledge, transferrable between distant regions. It was only necessary to acquire minimal limitational information (Rockman, 2003). Furthermore, camelids' migration patterns seem to have been quite different during the Late Pleistocene. The representation of different-aged segments in archaeological assemblages suggests the presence of stable guanaco family groups throughout the year in the intermediate floors (adult males and females, calves, and juveniles born the previous year before they are expelled from the group) (Cartajena, 2003). In the case of vicuñas, it is not possible to state whether they were present or if they were transported from the high puna (Cartajena, 2003; Cartajena et al., 2006). Either way, the greater humidity seems to have supported more stable faunal resources in the intermediate floors which were less affected by seasonality patterns, even attracting extinct species (*Equidae*) and others that no longer inhabit the region such as deer (*Hippocamelus antisensis*) (Cartajena, 2003).

Camelids continued to be the main source of subsistence during the Early Holocene, but some evidence suggests adjustment to more pronounced seasonal distribution and mobility (Cartajena et al., 2006). For instance, the high representation of adult individuals in sites such

as TU-68 and TA-1 point to prolonged occupations during the cold season. On the other hand, at TU-68 there is a remarkable frequency of Andean Doves (*Metriopelia* sp.), which nest in trees or rocky areas between April and August; while the presence of *Phoenicopterus* sp. in TU-67 and the high frequency of vicuñas in TA-1 could be the result of a more stable human access to the upper floors during summer. In addition to birds, other complementary local resources were important – such as vizcacha (*Lagidium viscacia*) which have crepuscular habits and frequent steep rocky areas in ravines of the pre-puna, and fossorial rodents like *Abrocoma* and *Ctenomys fulvus* that live in sandy environments of the desert lowlands.

## 8. Lithic technology and landscape learning

### 8.1. Scouting camps and lithic assemblages

For hunter-gatherers, lithic technology is closely linked to mobility, hence the lithic record gives us clues to understand how they learned the landscape as they moved about in it. There is a particular group of assemblages with a very low abundance of artefacts (SL-1, TU-109/T-1, Tam-2/4a, TUI-1 and SPN-6) (Fig. 9). This appears to be not merely a sampling issue, since an obvious technological pattern stands out: these assemblages are mainly composed of small flakes detached during the maintenance and use of retouched tools. Such tools were often made on distant raw materials such as obsidian or siliceous rocks, and were apparently already finished when they entered the sites. After occupation ended, they were transported back by their owners as part of their personal equipment. This would explain why the tools themselves are mostly absent, while their by-products are present. Just a few projectile points, knives and side-scrapers have been recovered in some of these sites, either broken or quite exhausted. Immediately available coarse-grain rocks from the area surrounding the settlement were used as sharp-edged tools. Bone remains and hearths are also recurrently found together with the lithic artefacts. Undoubtedly, hunting and primary processing of camelids were the central activities, although there was also some *in situ* consumption.

Everything seems to indicate that these small occupations were used only briefly as specialised-task sites within a wider settlement system; certainly, long-distance logistical mobility would fit quite well with this archaeological signature. Several of these sites also have very early dates that long precede the more stable residential camps in each locality. It may therefore be assumed that occupations of this kind allowed hunters from remote areas to explore and scout the landscape as part of hunting trips. In Tam-2/4a, for instance, just a few retouching flakes of an extra-local obsidian were recovered in a peat layer, constituting the first incursion so far known into the desert lowlands. The same applies to TU-109/T-1, where the oldest date for Tulán ravine and one of the earliest for the area was recorded. Despite their excellent quality and proximity, local raw materials such as Tulán tuff and grey obsidian are completely absent. In fact, the presence of green felsite could indicate a link with the Tuina area, more than 130 kilometres away.

The other sites show a similar pattern and early dates, but with more redundant use, or for longer periods. SPN-6 is an open-air hunting stop used at least twice; a few exhausted tools, an unmodified agate and flakes employed for primary processing and consumption of camelids were discarded after use around an exposed hearth (Fig. 11A and B). SL-1 was also reoccupied intermittently, presenting very low abundance throughout the entire sequence and interrupted by long gaps when it was abandoned. Conversely, in TUI-1 there are no visible periods of abandonment and the abundance and diversity of artefacts (some of them made on local obsidian) indicate greater occupational intensity. TU-109/E-IV is a later occupation in the eastern sector of the TU-109 rock shelter; it allows us to appreciate how the local landscape had been learned by then: beside the greater abundance and diversity of artefacts, local Tulán tuff and grey obsidian clearly predominate (Fig. 9).

### 8.2. Lithics, information and networking

Many of the social interactions in which lithic artefacts were involved occurred in the base camps like TA-1, SI-7, SPN-1 and SPN-20. The occupational redundancy and frequency of such interactions led to high discard rates, forming dense lithic assemblages scattered over large areas. Immediately available rocks procured during daily foraging activities were most

often used; they were transported to the camps in bulk in the form of cores or blanks. Thus, almost all the phases of the operational chains were carried out, from production through use to final discarding. The diversity of the toolkits also indicates that multiple tasks were carried out, linked to primary and secondary processing of animals, plants and mineral resources. In TUI-5, AC-1, SM-4, TUY-1, TU-67 and TU-68, although they are also medium-size occupations, the diversity and classes of tool (and other complementary evidence) suggest the performance of more specialized tasks.

A plausible scenario to explain size and functional discrepancies is the existence of seasonal fission/fusion strategies. Periodic macro-band aggregations would be a very auspicious context for acquiring and transmitting information. A certain homogeneity in lithic technology suggests sharing of technological knowledge. The clear predominance of the triangular, non-stemmed "Tuina" points, recorded in several sites in the south-central Andes, could be a good example (Fig. 12A). Other projectile points such as fishtail (Fig. 12C), although they are an unusual find in the Atacama Desert, are distributed throughout the whole of South America. Other shared patterns are also reflected in production modes, for instance the selection of large angular flakes obtained from cores of low technical investment (Fig. 11J) as tool blanks, which are then subjected to high edge complementarity and retouch intensity (Fig. 11A, C and F). Likewise, the use of cores on flakes and specific techniques for recycling exhausted tools, such as inverse retouching or the production of intentional fractures.

Towards the Early Holocene, important changes occur in lithic technology. In the first place, the assemblages show greater tool diversity and specialization. Retouched tools present smaller sizes as well as lower edge complementarity (Fig. 11 G, D, H and I). Some types not previously recorded, such as drills (Fig. 11E), make up a large part of the assemblages, indicating the importance of other secondary processing activities. The same can be said of the profuse grinding technologies in TA-1 (Fig. 11K) and other sites located on the margins of the Tambillo paleowetland, where extensive grinding and gathering areas have been described. In the case of bifacial operative chains, new projectile point designs are incorporated, some requiring greater technical investment. The stemmed, barbed "Punta Negra" (Fig. 12B), although mostly superficial, are frequently found in sites dated around the first part of the Early Holocene, while other designs are more characteristic of the second part, e.g. pentagonal (Fig. 12G), tetragonal "San Martín" (Fig. 12D) and the triangular, non-stemmed "Tambillo" (Fig. 12F). A similar, and contemporary, pattern of projectile point diversification has been observed in northwestern Argentina, attributed to changes in hunting organization. It has been suggested that during the Pleistocene-Holocene transition long-distance individual hunting predominated, based on the use of weapons thrown with spear-throwers (*atlatl*), but that by the end of the Early Holocene a collective hunting strategy had been developed using short-range, hand-thrown spears (Aschero and Martínez, 2001). Collective hunts have been proposed in parallel for sites in the high puna (Núñez et al., 2005). The frequent presence of projectile points, knives and scrapers indicates that there was a strong emphasis on hunting activities and animal processing in these large, dense seasonal camps.

In a context of greater territorial circumscription, individuals spend more time away from the camps to acquire high-ranked resources. The inter-band aggregations outside the residential area, either for collective hunting in the high puna or plant-gathering in lowland oases, would encourage cooperation and the transmission of knowledge from the elders to the young. Lithic raw material sources are unlikely to have been an exception. Since apprentices require large amounts of raw material, learning takes place sporadically in those places (Piegot, 1990). Some bifacial operative chains, such as Punta Negra points, required learning of more elaborate technical skills through active tutoring, for example. The case of SM-4 is quite illustrative. A large quantity of tetragonal projectile points were produced on immediately available basalt; however, the majority were rejected due to knapping accidents or morpho-functional deviations, while others were manufactured with great skill. Such differences in levels of technical competence would be expected in an apprenticeship context.

The technological similarities of our study area with northwestern Argentina have led to the proposal of a "Tuina-Inca Cave" cultural complex (Aschero and Podestá, 1986). The identification of obsidian from the eastern slope of the Andes proves the existence of early contacts between the two areas, over distances exceeding 200 km, meaning that mountain

passes over the Andes were already known from an early period. Judging by the remarkable increase in extra-local obsidian transport, social contacts were more stable and frequent by the end of the Early Holocene. By intensifying their long-distance ties, groups also increased their access to landscape information to cope with environmental fluctuations. Given the great distances involved and the steep relief of the Andes, logistic mobility would be a more effective strategy to achieve such face-to-face interactions, for instance in the form of social visits between reciprocal partners or small expeditions with the objective (among many others) of acquiring information. The circulation of obsidian, mainly in the form of projectile points (Table 3), is quite suggestive. It has been argued for later periods that obsidians were used as tokens or exchange goods (Escola et al., 2016). This could explain the importance acquired by bifacial knapping at the end of the Early Holocene, and not only in terms of design diversity. The percentage of bifacial products and by-products in the assemblages is striking, often involving more elaborate thinning and final shaping procedures.

## 9. Discussion

### 9.1 A gradual process?

The evidence to date shows that Late Pleistocene occupations (13,000 to 11,500 cal BP) were limited exclusively to the pre-puna floor (2700-3200 masl), indicating that hunter-gatherers selected the more productive and legible habitats available on this floor in the initial stages of dispersion into the area. The high puna and desert lowlands were only included in the settlement process later, at the end of the Early Holocene. However, we cannot infer a positive linear relationship between landscape learning on the one hand and diversity of inhabited environments on the other. The synchrony between prolonged droughts and different abandonment and relocation events suggests a more complex scenario, perhaps better described as a process of learning and experimentation with local resources. After the abandonment of the pre-puna, this process culminated in complementary land-use of the highlands and lowlands – paradoxically, the two areas considered more risky. This structured pattern of seasonal mobility did not simply allow groups to exploit efficiently the environmental variations of the annual cycle; combined with more specialized technologies, it was a key strategy for dealing with climate change.

However, if we compare this colonization process with that in neighbouring areas, we detect important differences in timing. In the northern Atacama (Osorio et al., 2017), northwestern Argentina (Yacobaccio et al., 2017) and the Bolivian altiplano (Capriles and Albarracín-Jordan, 2013), occupation of the high puna occurred substantially earlier, and the same appears to be true of the lowlands, based on information from the sites in the Pampa del Tamarugal (Latorre et al., 2013). Why is there no record of previous occupations in the south-central Atacama outside the prepuna floor? There are two possibilities: either these areas were indeed colonized later due to adverse conditions for human subsistence, or there are problems of visibility and conservation of the archaeological record. According to Núñez et al. (2002), the earliest occupations located on the margins of high altitude lakes before they reached their maximum dimensions may have been buried by sediments. The low sedimentation rate and wind erosion represent recurrent problems in these archaeological contexts. Undoubtedly, early incursions could have taken place, but they are difficult to detect in a time-averaged, superficial archaeological record. A large number of human occupations attributed to the Early Archaic have still not been dated.

Although the peopling process could be “gradual” in terms of timing and the diversity of inhabited environments, evidence suggests that the hunter-gatherer groups maintained a way of life already adapted to the salt puna (Núñez and Santoro, 1989; Núñez et al., 2002; Aschero, 2010). At least, there is no evidence to support peopling from the coast – on the contrary, early human dispersion was facilitated by transferable prior knowledge, based on the hunting of camelids and the collection of plants in azonal formations. In their search for richer resources, these groups may have followed dispersion routes through the Andes, tracking megapatches which were more homogeneous than current biomes (Cartajena et al., 2014, Osorio et al., 2017, Loyola et al., 2018).

### 9.2 Learning to move, moving to learn



During human dispersal into an empty land mass, mobility is practically unfettered; however, arid landscapes pose a special problem for human settlement due to water scarcity. The location patterns of residential camps indicate that placement selection was strongly conditioned by the distribution, availability and quality of fresh water, even during wet climatic conditions. Like many hunter-gatherer groups in desert environments, the first human groups could have followed a "tethered" foraging pattern (Kelly, 2013:93) in which knowledge about the location of the better quality waterholes and recharge cycles was critical for programming mobility (Gould, 1991; Marlowe, 2010; Hiscock and Ebert, 2011). However, the contribution of plant as buffer water reserves should not be ruled out (Silberbauer, 1981). The remains of roots and tubers found in SL-1 could be evidence of such strategy.

Several authors have proposed the existence of high residential mobility during the early peopling of the Atacama puna (Núñez et al., 2002; Aschero, 2010; Yacobaccio and Morales, 2013). Indeed, the abandonment and relocation events recorded in the study sites associated with prolonged droughts could be the result of high residential mobility and more flexible territorial patterns. Foragers in environments with high interannual variations in rainfall employ an "escape and evasion" strategy (Gould, 1991) and constant migrations (Silberbauer, 1981; Cashdan, 1984; Tanaka, 1980). However, settlement patterns and archaeological assemblages point to the existence of complementary logistical mobility. Following Aldenderfer (2006), this could be due to the emergence of more structured foraging patterns in high altitude environments, leading to a decrease in residential movements. Recently, attention has been drawn to the occupation of logistical camps on the high puna floor of neighbouring areas (Capriles et al., 2013; Osorio et al., 2017).

Residential mobility allowed groups to disperse quickly over a large, continuous area; however, it reduced the possibilities of acquiring extensive information on the landscape, especially considering that site location was tied to the distribution of water sources. In a context of incongruous resources or "separate habitats", logistical mobility was a useful solution, also offering better possibilities of capturing environmental information. The interaction of these two mobility strategies had important consequences for the peopling process. When new patches were incorporated into the logistics radius, changes were triggered in residential mobility circuits and new residential camps were attracted.

### 9.3 Hidden networks and encrypted information

The idea that first human groups of the salt puna were relatively autonomous and maintained highly dispersed social networks has predominated. However, our data suggest that these small, scattered bands managed to sustain social cohesion at the supra-band level and maintain long-distance contacts. Low population density is good way to maintain an adequate immediate return in an environment of low primary productivity, but in the long term it is not demographically viable (Wobst, 1974). If we judge from the differences in the size of the sites and their functional orientations, the occurrence of periodic inter-band aggregations is an eminently possible scenario. A flexible social organization and fluid membership (as part of fusion-fission strategies, for example) would allow to maintain small group sizes while remaining closely interconnected within exogamic networks, ensuring reproductive success and information transmission. However, inferring social aggregations from the archaeological record is always complex (Hoffman, 1994). Other archaeological indicators besides lithic technology will certainly be necessary in future.

How extensive these networks were is just as difficult to establish. Obsidian transport suggests the existence of interaction networks across the 300 km. This is not unusual in small-scale forager bands; indeed, some authors suggest that as the size of the group decreases, the distances travelled to visit neighbouring groups in order to find a mate increases proportionally (MacDonald, 1998). We have suggested the hypothesis that many of these obsidian objects circulated in the form of projectile points as exchange goods, which correlates with hunter-gatherer ethnography (Hiscock and Ebert, 2011). However, there are no reliable archaeological indicators to distinguish indirect procurement through exchange from direct long-distance procurement. Furthermore, what is assumed to be an exchange could in fact be the result of a wide diversity of behaviours and different forms of social interaction (Bruch, 1988), each of

which prints particular signatures in the archaeological record. More detailed technological studies on the circulation patterns of lithic raw materials will provide new perspectives, but for now the existence of generalized technologies with a certain regional homogeneity can give us an idea about the spatial scale of information flows.

Apparently, social contacts were not limited only to the highlands; the coastal area inhabited contemporaneously by the Huentelauquén cultural tradition (Salazar et al., 2017) also seems to have formed part of early interaction networks. Conch shells from the Pacific coast (*Olivia peruviana*, *Concholepas concholepas* and *Argopecten purpuratus*) have been recorded in Early Holocene sites, including TU-67, TU-109/E-IV and TA-1 (Núñez et al., 2005). Other evidence can be found in the similarity of the funerary practices observed in TA-1 (Costa-Junqueira et al., 2001). The intensification and expansion of long-distance interactions at the end of the Early Holocene could be a valid strategy for coping with increased aridity and resource failure, offering a safety net (Whallon, 2006), especially in a context of increasingly contrasting habitats and decreased mobility (Cashdan, 1984; Barnard, 1992). Ultimately, these early interaction networks structured the peopling process itself, facilitating the circulation of resources, people and information. They formed the basis for the emergence of later cultural traditions and social complexity.

## 10. Conclusions

The highlands of the Atacama Desert probably represent one of the most challenging environments for human colonization, so their peopling was necessarily a gradual process, structured over time as human groups learned this arid landscape. Knowing “what it’s like out there” was a critical and permanent task. Rather than a constant southward movement in the sense of a biogeographic corridor, on a millennial-centennial scale, populations dispersed progressively and selectively at different rhythms and speeds, based on their increasing knowledge of a changing environment. Scouting as part of logistical hunting parties and information-pooling through networking were essential complementary strategies to acquire and transmit information about climate regimes, routes and resources.

Late Pleistocene occupations were initially limited to the pre-puna floor, which offered an intermediate habitat between the extreme conditions of the high puna and the desert lowlands. On this altitude floor, the more humid climate generated productive micro-environments with less acute resource incongruence and less extreme seasonality. The greater legibility and lower information demand encouraged rapid dispersal from other neighbouring eco-regions with a similar ecological structure. Generic prior knowledge based on camelid hunting and plant collection in azonal formations could be applied successfully. However, the progressive imposition of an arid climate during the Early Holocene in the form of prolonged droughts motivated events of abandonment, relocation and incorporation of previously inhabited areas. In the long term, this led to the abandonment of most of the pre-puna sites and the occupation of the high puna and the desert floor.

The end of the Early Holocene was a period of deep transformations in social organisation. Technological changes reflect not only experimentation and learning on local resources but also the production of technologies to connect people in time and space, allowing the transmission of information. The complementary land-use of the highlands and desert lowlands was the result of a long process of landscape learning, which allowed to counteracted the greater spatio-temporal resource incongruence. In the long term, such transformations laid the foundations for an economic rationale which would form the basis of early social complexity in the region, and which persists down to the present.

## 11. Acknowledgments

We thank Francisca Santana and Mauricio Uribe for inviting us to present this work in the 2017 session of SAA, and to publish it in this volume. We also thank the anonymous reviewers for all their comments and suggestions. We thank Wilfredo Faúndez and Rodrigo Lorca for photographic support and Frank Haddon for his invaluable comments.

## 12. Referenced

1. Aldenderfer, M., 2006. Modelling Plateau Peoples: The Early Human Use of the World's High Plateaux. *World Archaeology* 38:357–370.
2. Aldunate, C., Armesto, J., Castro, V., Villagrán, C., 1981. Estudio Etnobotánico en una Comunidad Precordillerana de Antofagasta: Toconce. *Boletín del Museo Nacional de Historia Natural* 38, 183-223.
3. Arroyo, M., Squeo, F., Armesto, J., Villagrán, C., 1988. Effects of aridity on plant diversity in the northern Chilean Andes: Results of a natural experiment. *Annals of Missouri Botanical Garden* 75: 55-78.
4. Aschero, C., 2010. Arqueología de Puna y Patagonia Centro Meridional: Comentarios Generales y Aporte al Estudio de los Cazadores Recolectores Puneños en los Proyectos dirigidos desde el IAM (1991-2009). In: Arenas, P., Aschero, C., Tobaoda, C. (Eds.), *Rastros en el Camino... Trayectos e Identidades de una Institución. Homenaje a los 80 años del IAM-UNT*, EDUNT Editorial, San Miguel de Tucumán, pp. 257-293.
5. Aschero, C., Podestá, M., 1986. El arte rupestre en asentamientos precerámicos de la Puna Argentina. *Runa* 16: 29-57.
6. Aschero, C., Martínez, J., 2001. Técnicas de caza en Antofagasta de la Sierra. *Relaciones de la Sociedad Argentina de Antropología* 26, 215-241.
7. Barnard, A., 1992. *Hunters and herders of Southern Africa: a comparative ethnography of the Khoisan peoples*. Cambridge: Cambridge University Press.
8. Beaton, J., 1991. Colonizing continents: Some problems from Australia and the Americas. In: Dillehay, T.E., Meltzer D.J. (Eds.), *The First Americans: Search and Research*. CRC Press, Boca Raton, Florida, pp. 209-230.
9. Betancourt, J.L., Latorre, C., Rech, J.A., Quade, J., Rylander, K.A., 2000. A 22.000 Year Record of Monsoonal Precipitation from Northern Chile's Atacama Desert. *Science* 289 (5484), 1542-1546.
10. Binford, L.R., 2001. *Constructing Frames of Reference. An Analytical Method for Archaeological Theory Building using Ethnographic and Environmental Data Sets*. University of California Press, Berkeley.
11. Bobst, A.L., Lowenstein, T.K., Jordan, T.E., Godfrey, L.V, Ku, T.-L., Luo, S., 2001. A 106 ka paleoclimate record from drill core of the Salar de Atacama, northern Chile. *Palaeogeography, Palaeoclimatology, Palaeoecology* 173, 21-42.
12. Bronk Ramsey, C., 2017. OxCal 4.3 manual, [http://c14.arch.ox.ac.uk/oxcalhelp/hlp\\_contents.html](http://c14.arch.ox.ac.uk/oxcalhelp/hlp_contents.html)
13. Burch, E., 1988. Modes of Exchange in North West Alaska. En: T. Ingold, D. Riches, y J. Woodburn (Eds.), *Hunters and Gatherers, 2, Property, Power and Ideology*, Berg, Oxford, pp. 95-109.
14. Capriles, J.M., Albarracín-Jordan, J., 2013. The earliest human occupations in Bolivia: A review of the archaeological evidence. *Quatern. Int.* 301:46-59.
15. Cartajena, I., 2003. *Los conjuntos arqueofaunísticos del Arcaico Temprano en la Puna de Atacama, Norte de Chile*. Ph.D thesis, Freie Universität Berlin, Germany.
16. Cartajena, I., Núñez, L., Grosjean, M., 2006. Las Arqueofaunas del Arcaico Temprano en la vertiente occidental de la Puna de Atacama. In: *Sociedad Chilena de Arqueología (Eds.), Actas del XVI Congreso Nacional de Arqueología Chilena*, Museo de Historia Natural de Concepción, Ediciones Escaparate, Concepción, pp. 507-517.
17. Cartajena, I., Loyola, R., Núñez, L., Faúndez, W., 2014. Problemas y Perspectivas en la interpretación del Registro Espacial de Punta Negra Imilac. In: Falabella, F., Sanhueza, L., Cornejo, L., Correa, I. (Eds.), *Distribución Espacial en Sociedades no Aldeanas: del Registro Arqueológico a la Interpretación Social*, Serie Monográfica de la Sociedad Chilena de Arqueología 4, Santiago, pp. 143-162.
18. Cashdan, E., 1984. G||ana Territorial Organization. *Human Ecology*, 12(4): 443-463.
19. Costa-Junqueira, M., 2001. Modalidades de enterramientos Humanos Arcaicos en el Norte De Chile. *Chungará* 33(1), 55-62.
20. De Souza, P., 2004. Cazadores Recolectores del Arcaico Temprano y Medio en la Cuenca Superior del río Loa: Sitios, Conjuntos líticos y Sistemas de asentamiento. *Estudios Atacameños* 27: 7-43.
21. DGA, 2004. Actualización delimitación de acuíferos que alimentan vegas y bofedales, región de Antofagasta. Final report. Departamento de Estudios y Planificación-Dirección General de Aguas, Santiago.
22. Escola, P., Hocsman, S., Babot, M., 2016. Moving obsidian: The case of Antofagasta de la Sierra basin (Southern Argentinean Puna) during the late Middle and Late Holocene. *Quaternary International* 422,109-122.
23. Fiedel, S. J., Anthony, D. W., 2003. Deerslayers, pathfinders, and icemen: Origins of the European Neolithic as seen from the frontier. In *Colonization of Unfamiliar Landscapes: The Archaeology of Adaptation*, M. Rockman and J. Steele, eds. London: Routledge, 144– 168.

24. Fitzhugh, B., Phillips, S. C., Gjesfjeld, E., 2011. Modeling variability in hunter-gatherer information networks: An archaeological case study from the Kuril Islands. In: Whallon, R., Lovis, W. A., Hitchcock, R. K. (Eds.), *Information and its role in hunter-gatherer bands*, Los Angeles: UCLA/Cotsen Institute of Archaeology Press, pp. 85-115.
25. Ford, A., 2011. Learning the Lithic Landscape: Using Raw Material Sources to Investigate Pleistocene Colonisation in the Ivane Valley, Papua New Guinea. *Archaeol. Oceania* 46(2), 42-53.
26. Franklin, W.L., 1982. Biology, ecology, and relationship to man of the South American camelids. *Special Publication Pymatuning Laboratory of Ecology* 6, 457-489.
27. Fritz, P., Silva, C., Suzuki, O., Salati, E., 1979. Isotope hydrology in Northern Chile. In: IAEA (Eds.), *Isotope hydrology 1978: Proceeding of an international symposium on isotope hydrology vol 2*, Vienna, pp. 525-543.
28. Gamble, C., 1993. Exchange, Foraging and Local Hominid Networks. In: Scarre, C., Healy, F. (Eds.), *Trade and Exchange in Prehistoric Europe*, Oxford, pp. 35-44.
29. Gamble, C., 1994. *Timewalkers. The Prehistory of Global Colonization*. Harvard University Press, Cambridge.
30. Gamble, C., 1995. Large Mammals, Climate and Resource Richness in Upper Pleistocene Europe. *Acta Zoologica Cracova* 38(1),155-75.
31. Garreaud, R.D., Vuille, M., Clement, A.C., 2003. The climate of the Altiplano: observed current conditions and mechanisms of past changes. *Palaeogeography, Palaeoclimatology, Palaeoecology* 194, 5-22.
32. Gayó, E.M., Latorre, C., Jordan, T.E., Nester, P.L., Estay, S.A., Ojeda, K.F., Santoro, C.M., 2012. Late Quaternary hydrological and ecological changes in the hyperarid core of the northern Atacama Desert (~21°S). *Earth-Science Reviews* 113, 120-140.
33. Geyh, M., Grosjean, M., Núñez, L., Schotterer, U., 1999. Radiocarbon Reservoir Effect and the Timing of Late Glacial/Early Holocene Humid Phase in the Atacama Desert (Northern Chile). *Quaternary Research* 52, 143-153.
34. Golledge, R.G., 1999. Human Wayfinding and Cognitive Maps. in R.G. Golledge (ed.) *Wayfinding Behavior: Cognitive Mapping and Other Spatial Processes*, Baltimore: Johns Hopkins University Press.
35. Golledge, R.G., 2003. Human Wayfinding and Cognitive Maps. In: Rockman, M., Steele, J., (Eds.), *Colonization of Unfamiliar Landscapes: The Archaeology of Adaptation*. London: Routledge, pp 25-43.
36. Gould, R.A., 1991. Arid land foraging as seen from Australia – adaptive models and behavioural realities. *Oceania* 62:12-33.
37. Grosjean M., Van Leeuwen, J., Van der Knaap, W., Ammann, B., Tanner, W., Messerli, B., Núñez, L., Valero-Garcés, B., Veit, H., 2001. A 22,000 14C year BP Sediment and Pollen Record of Climate Change of Laguna Miscanti (23°S), Northern Chile. *Global and Planetary Change* 28, 35-51.
38. Grosjean, M. Cartajena, I. Geyh, M. A., Núñez, L., 2003. From Proxy-data to Palaeoclimate Interpretation: The Mid-Holocene Paradox of the Atacama Desert, Northern Chile. *Palaeogeography, Palaeoclimatology, Palaeoecology* 194, 247-258.
39. Grosjean, M., Núñez, L., Cartajena, I., 2005. Palaeoindian occupation of the Atacama Desert, northern Chile. *Journal of Quaternary Science* 20, 643-653.
40. Hegmon, M., Fisher, L.E., 1991. Information strategies in hunter-gatherer societies. In: Miracle, P. T., Fisher, L. E., Brown, J. (Eds.), *Foragers in Context: Long-Term, Regional, and Historical Perspectives in Hunter-Gatherer Studies*. Michigan Discussions in Anthropology, Department of Anthropology, University of Michigan, Ann Arbor, pp. 127-145.
41. Hitchcock, R., Ebert, J., 2011. Where is That Job? Hunter-Gatherer Information Systems in Complex Social Environments in the Eastern Kalahari Desert, Botswana. In: Whallon, R., Lovis, W., Hitchcock, R. *The Role of Information in Hunter-Gatherer Bands*. Los Angeles: UCLA/Cotsen Institute of Archaeology Press, pp. 133-166.
42. Hofman, J.L., 1994. Paleoindian aggregations on the Great Plains. *Journal of Anthropological Archaeology* 13:341-70.
43. Hogg, A., Hua, Q., Blackwell, P., Niu, M., Buck, C., Guilderson, T., Heaton, T., Palmer, J., Reimer, P., Reimer, R., Turney, C., Zimmerman, S., 2013. SHCal13 Southern Hemisphere calibration, 0-50,000 years cal BP. *Radiocarbon* 55(4),1889-903.
44. Houston, J., 2006a. Variability of precipitation in the Atacama Desert: its causes and hydrological impact. *International Journal of Climatology* 26, 2181-2198.
45. Houston, J., 2006b. The great Atacama flood of 2001 and its implications for Andean hydrology. *Hydrological Processes* 20, 591-610.
46. Jochim, M.A., 1976. *Hunter-Gatherer Subsistence and Settlement*. Academic Press, New York.
47. Kelly, R.L., 1995. *The Foraging Spectrum: Diversity in Hunter-Gatherer Lifeways*. Smithsonian Institution Press, Washington DC.

48. Kelly, R.L., 2003. Colonization of New Land by Hunter-Gatherers: Expectations and Implications Based on Ethnographic Data. In: Rockman, M., Steele, J., (Eds.), *Colonization of Unfamiliar Landscapes: The Archaeology of Adaptation*, Routledge, London, pp. 44–58.
49. Kelly, R.L., 2013. *The Lifeways of Hunter-Gatherers: The Foraging Spectrum*. Cambridge University Press, Cambridge.
50. Kelly, R.L., Todd, L.C., 1988. Coming into the Country: Early Paleoindian Hunting and Mobility. *American Antiquity* 53(2), 231–44.
51. Kull, C., Grosjean, M., 1998. Albedo Changes, Milankovitch forcing, and late Quaternary climate Changes in the Central Andes. *Climate Dynamics* 14, 871–88.
52. Latorre, C., Betancourt, J. L., Rylander, K. A., Quade, J., 2002. Vegetation Invasions into the Absolute Desert: a 45000 yr rodent Midden Record from the Calama-Salar de Atacama Basins, Northern Chile (lat 22°-24° S). *Geological Society of America Bulletin* 114(3), 349-366.
53. Latorre, C., Betancourt, J.L., Rylander, K.A., Quade, J., Matthei, O., 2003. A 13.5-kyr vegetation history from the arid prepuna of northern Chile (22–23°S). *Palaeogeography, Palaeoclimatology, Palaeoecology* 194, 223–246.
54. Latorre, C., J. Betancourt, M. Arroyo., 2006. Late Quaternary Vegetation and Climate History of a Perennial River Canyon in the Río Salado Basin (22°S) of Northern Chile. *Quaternary Research* 65: 450- 466.
55. Latorre, C., Santoro, C.M., Ugalde, P.C., Gayo, E.M., Osorio, D., Salas-Egaña, C., De Pol-Holz, R., Joly, D., Rech, J.A., 2013. Late Pleistocene human occupation of the hyperarid core in the Atacama Desert, northern Chile. *Quaternary Science Reviews* 77, 19–30.
56. Lovis, W.A., Donahue, R.E., Holman, M.B., 2005. Long-distance logistic mobility as an organizing principle among northern hunter-gatherers: a great lakes middle holocene settlement system. *American Antiquity* 70, 669–693.
57. Loyola, R., Núñez, L., Aschero, C., Cartajena, I., 2017. Tecnología Lítica del Pleistoceno Final y la Colonización del Salar de Punta Negra (24,5° S), Desierto de Atacama. *Estudios Atacameños* 55, 5-34.
58. Loyola, R., Cartajena, I., Núñez, L., López, P., 2018. Moving into an arid landscape: Lithic technologies of the Pleistocene-Holocene transition in the high-altitude basins of Imilac and Punta Negra, Atacama Desert. *Quaternary International* 473, 206-224.
59. MacDonald, D.H., 1998. Subsistence, Sex, and Cultural Transmission in Folsom Culture, *Journal of Anthropological Archaeology* 17:217–39.
60. Maldonado, A., Betancourt, J.L., Latorre, C., Villagrán, C., 2005. Pollen analyses from a 50,000-yr rodent midden series in the southern Atacama Desert (25°30'S). *Journal of Quaternary Science* 20, 493–507.
61. Marlowe, F., 2010. *The Hadza Hunter-Gatherers of Tanzania*. Berkeley: University of California Press.
62. Meltzer, D.J., 2002. What do you do when no one's been there before? Thoughts on the exploration and colonization of newlands. In: Jablonski, N. (Ed.), *The First Americans: The Pleistocene Colonization of the New World*. California Academy of Sciences, San Francisco.
63. Meltzer, D.J., 2003. Lessons in Landscape Learning. In: Rockman M., Steele, J., (Eds.), *Colonization of Unfamiliar Landscapes. The Archaeology of Adaptation*, Routledge, New York, pp. 222-241.
64. Meltzer, D.J., 2004. On Possibilities, Prospecting, and Patterns. Thinking about a Pre-LGM Human Presence in the Americas. In: Madsen, D.B., (Ed.), *Entering America. Northeast Asia and Beringia before the Last Glacial Maximum*. The University of Utah Press, Salt Lake City, pp. 359–377.
65. Meltzer, D.J., 2009. *First Peoples in a New World. Colonizing Ice Age America*. University of California, Berkeley.
66. Messerli, B., Grosjean, M., Bonani, G., Bürgi, A., Geyh, M. A., Graf, K., Ramseyer, K., Romero, H. Schotterer, U., Schreier, H., Vuille, M., 1993. Climate Change and Dynamics of Natural Resources in the Altiplano of Northern Chile During Late Glacial and Holocene times. First synthesis. *Mountain Research and Development* 13(2), 117-127.
67. Milne, S.B., 2014. Landscape Learning and Lithic Technology: Seasonal Mobility, Enculturation, and Tool Apprenticeship among the Early Palaeo-Eskimos. In: Cannon, A. (Ed.), *Structured Worlds: The Archaeology of Hunter-Gatherer Thought and Action*. London: Equinox Publishing Ltd., pp. 95-115.
68. Nester, P.L., Gayo, E., Latorre, C., Jordan, T.E., Blanco, N., 2007. Perennial stream discharge in the hyperarid Atacama Desert of northern Chile during the latest Pleistocene. *Proceedings of the National Academy of Sciences* 104, 19724–19729.
69. Nieves, M., Stoffle, R., 2003. Tracking the Role of Pathways in the Evolution of a Human Landscape: The St. Croix Riverway in Ethnohistorical Perspective. In: Rockman, M., Steel, J., (Eds.), *Colonization of Unfamiliar Landscapes: The Archaeology of Adaptation*. Routledge, London, pp. 59–80.
70. Núñez, L., Santoro, C., 1989. Cazadores de la Puna Seca y Salada del Area Centro Sur Andina (Norte de Chile). *Estudios Atacameños* 9, 13-65.

71. Núñez, L., Grosjean, M., Cartajena, I., 2002. Human occupations and climate change in the Puna de Atacama, Chile. *Science* 298, 821-824.
72. Núñez, L., Grosjean, M., Cartajena, I., 2005. Ocupaciones humanas y paleoambientes en la Puna de Atacama. Universidad Católica del Norte-Taraxacum, San Pedro de Atacama.
73. Osorio, D., Steele, J., Sepúlveda, M., Gayo, E.M., Capriles, J.M., Herrera, K., Ugalde, P., De Pol-Holz, R., Latorre, C., Santoro, C.M., 2017. The Dry Puna as an ecological megapatch and the peopling of South America: Technology, mobility, and the development of a Late Pleistocene/Early Holocene Andean hunter-gatherer tradition in northern Chile. *Quaternary International* 461, 41-53.
74. Pfeiffer, M., Latorre, C., Santoro, C.M., Gayo, E.M., Rojas, R., Carrevedo, M.L., McRostie, V.B., Finstad, K.M., Heimsath, A.M., Jungers, C., De Pol-Holz, R., Amundson, R., 2018. Chronology, stratigraphy and hydrological modelling of extensive wetlands and paleolakes in the hyperarid core of the Atacama Desert during the late Quaternary. *Quaternary Science Reviews* 197, 224-245.
75. Pigeot, N., 1990. Technical and social actors in Prehistory. Flintknapping specialists and apprentices at Magdalenian Étiolles. *Archaeological Review from Cambridge*, 9 : 1, « Technology in the Humanities », Cambridge, pp.126-141.
76. Placzek, C., Quade, J., Betancourt, J., Patchett, P., Rech, J., Latorre, C., Matmon, A., Holmgren, C., English, N., 2009. Climate in the Dry central Andes over Geologic, Millennial, and Interannual Timescales. *Annals of the Missouri Botanical Garden* 96, 386-397.
77. Puig, S., Rosi, M.I., Videla, F., Méndez, E., 2011. Summer and winter diet of the guanaco and food availability for a High Andean migratory population (Mendoza, Argentina). *Mammalian Biology* 76, 727-734
78. Quade, J., Rech, J., Betancourt, J., Latorre, C., Quade, B., Rylander, K., Fisher, T., 2008. Paleowetlands and Regional Climate Change in the Central Atacama Desert, Northern Chile. *Quaternary Research* 69(3), 343-360.
79. Rech, J. A., Quade, J., Betancourt, J. L., 2002. Late Quaternary Paleohydrology of the Central Atacama Desert (lat 22-24°S), Chile. *Geological Society of America Bulletin* 114(3), 334-348.
80. Risacher, F., Alonso, H., Salazar, C., 1998. Geoquímica de Cuencas Cerradas, I, II y III Regiones. Final report. DGA-UCNORSTOM, Santiago.
81. Risacher, F., Alonso, H., Salazar, C., 2003. The origin of brines and salts in Chilean salars: a hydrochemical view. *Earth-Science Reviews* 63, 249-293.
82. Rockman, M., 2003. Knowledge and Learning in the Archaeology of Colonization. In: Rockman, M., Steele, J. (Eds.), *Colonization of Unfamiliar Landscapes: The Archaeology of Adaptation*, Routledge, Londres, pp. 3-24.
83. Rockman, M., 2009. Landscape learning in relation to evolutionary theory. In: Prentiss, A., Kuijt, I. Chatters, J.C. (Eds.), *Macroevolution in human prehistory*, Springer, New York, pp. 51-71.
84. Roebroeks, W., 2003. Landscape learning and the earliest peopling of Europe. In: Rockman, M., Steele, J. (Eds.), *Colonization of Unfamiliar Landscapes: The Archaeology of Adaptation*. Routledge, London, pp. 99-115.
85. Romero, H., Mendonca, M., Méndez, M. Smith, P., 2013. Macro y mesoclimas del Altiplano Andino y Desierto de Atacama: Desafíos y estrategias de adaptación social ante su variabilidad. *Revista de Geografía Norte Grande* 55, 19-41.
86. Sáez, A., Godfrey, L.V., Herrera, C., Chong, G., Pueyo, J.J., 2016. Timing of wet episodes in Atacama Desert over the last 15 ka. The Groundwater Discharge Deposits (GWD) from Domeyko Range at 25°S. *Quaternary Science Reviews* 145, 82-93.
87. Salazar, D., Arenas, C., Andrade, P., Olgúin, L., Torres, J., Flores, C., Vargas, G., Rebolledo, S., Borie, C., Sandoval, C., Silva, C., A. Delgado, Lira, N., Robles, C., 2018. From the use of space to territorialisation during the Early Holocene in Taltal, coastal Atacama Desert, Chile. *Quaternary International* 473: 225-241.
88. Santoro, C., Latorre, C., Salas, C., Osorio, D., Ugalde, P., Jackson, D., Gayó, E., 2011. Ocupación Humana Pleistocénica en el Desierto de Atacama. *Primeros Resultados de la Aplicación de un Modelo Predictivo Interdisciplinario*. *Chungara* 43, 353-366.
89. Seleenfreund, A., Pino, M., Glascok, M., Sinclair, C., Miranda, P., Pasten, D., Cancino, S., Dinator, M.I., Morales, J.R., 2010. Morphological and Geochemical Analysis of the Laguna Blanca/ Zapaleri Obsidian Source in the Atacama Puna. *Geoarchaeology* 25, 245-263.
90. Silberbauer, G., 1981. *Hunter and habitat in the central Kalahari desert*. University Press, Cambridge.
91. Squeo, F. A., Cavieres, L., Arancio, G., Novoa, J. E., Matthei, O., Marticorena, C., Rodríguez, R., Arroyo, MTK, Muñoz, M., 1998. Biodiversidad de la flora vascular en la región de Antofagasta, Chile. *Revista Chilena de Historia Natural* 71: 571-591
92. Steele, J., Rockman, M., 2003. Where do we go from here? Modelling the Decision Making Process During Exploratory Dispersal. In: Rockman, M., Steele, J. (Eds.), *Colonization of Unfamiliar Landscapes: The Archaeology of Adaptation*. Routledge, London, pp. 130-143.

93. Tanaka, J., 1980. *The San, hunter-gatherers of the Kalahari: a study in ecological anthropology*. Tokyo: University of Tokyo Press.
94. Tolan-Smith, C., 2003. The Social Context of Landscape Learning and the Lateglacial – Early Postglacial Recolonization of the British Isles. In: Rockman, M., Steele, J. (Eds.), *Colonization of Unfamiliar Landscapes: The Archaeology of Adaptation*, Routledge, London, pp. 116–129.
95. Villagrán, C., Castro, V., 1997. Etnobotánica y manejo ganadero de las vegas, bofedales y quebradas en el Loa superior, Andes de Antofagasta, II Región. *Chungará* 29, 275-304.
96. Villagrán, C., Armesto, J., Arroyo, M., 1981. Vegetation in a High Andean Transect Between Turi and Cerro León in Northern Chile. *Vegetatio* 48, 3-16.
97. Villagrán, C., Castro, V., Sánchez, G., Romo, M., Latorre, C., Hinojosa, L.F., 1998. La tradición surandina del desierto: Etnobotánica del área del Salar de Atacama (Provincia de El Loa, Región de Antofagasta, Chile). *Estudios Atacameños* 16, 7-105.
98. Vuille M, Ammann, C., 1997. Regional snowfall patterns in the high, arid Andes. *Climate Change* 36, 413-423.
99. Walthall, J.A., 1998. Rockshelters and Hunter-Gatherer Adaptation to the Pleistocene/Holocene Transition. *American Antiquity* 63(2): 223-238.
100. Whallon, R., 2006. Social networks and information: non-“utilitarian” mobility among hunter-gatherers. *Journal of Anthropological Archaeology* 25, 259-270.
101. Whallon, R., 2011. An Introduction to Information and Its Role in Hunter-Gatherer Bands. In: Whallon, R., Lovis, W.A., Hitchcock, R.K., (Eds.), *Information and Its Role in Hunter-Gatherer Bands*, Cotsen Institute of Archaeology Press, Los Angeles, pp. 1–27.
102. Wobst, H. M., 1974. Boundary conditions for Paleolithic social systems: A simulation approach. *American Antiquity*, 39: 147–178
103. Wren, C.D., Costopoulos, A., 2015. Does Environmental Knowledge Inhibit Hominin Dispersal? *Human Biology* 87, 205–223.
104. Yacobaccio, H.D., 2017. Peopling of the high Andes of northwestern Argentina. *Quaternary International* 461,34-40.
105. Yacobaccio, H.D., Morales, M.R., 2013. Ambientes pleistocénicos y ocupación humana temprana en la Puna Argentina. *Boletín de Arqueología PUCP* (15), 337-356.
106. Yacobaccio, H.D., Escola, P.S., Pereyra, F.X., Lazzari, M., Glascock, M.D., 2004. Quest for ancient routes: obsidian sourcing research in Northwestern Argentina. *Journal of Archaeological Science* 31, 193-204.

## Figures titles

Figure 1. Landscape variability of the south-central Atacama highlands: (A) Tuyajto lake (4000 masl); (B) Tulán river (3000 masl); (C) Tambillo desert lowlands (2200 masl).

Figure 2. Geographic location of south-central Atacama

Figure 3. Archaeological sites and environmental setting of the south-central Atacama: (A) Geomorphological morphostructural units; (B) Zonal vegetation belts (after Villagrán et al., 1998); (C) Geomorphological profile (22°S).

Figure 4. Paleoenvironmental and Paleoclimatic local records: (A) Estimated lake levels of Miscanti Lake (22°45 S, 4140 masl) (asterisk indicates a dry period) (Grosjean et al., 2001); (B) Groundwater discharge levels of Tilomonte wetlands (23.5°S, 2550-2600 masl) (Rech et al., 2002); (C) Water table levels of Imilac-Punta Negra (Quade et al., 2008) (24-24.5°S, 2900-3000 masl); (D) Rodent midden records of the Atacama basin (22-23°S, 3100-3300 / 2400-3200 masl) (Latorre et al., 2003).

Figure 5. Archaeological sites: (A) TUI-5; (B) SPN-19/20; (C) TU-109; (D) TUY-1; (E) TA-1; (F) TUI-1.

Figure 6. Human events and climatic conditions: (A) <sup>14</sup>C dates (cal. BP) by elevation (masl); (B) Summed probability distributions. Dates have been calibrated with OxCal 4.3.2 (Bronk Ramsey, 2017) using the ShCal13 curve (Hogg et al., 2013).

Figure 7. Inferred pathway networks and placement patterns of archaeological sites

Figure 8. Site areas and available resources in a radius of 20 km.

Figure 9. Lithic raw materials distribution by site

Figure 10. Taxonomic diversity represented in TUI-5 (E-IV) (from Cartajena, 2003).

Figure 11. Retouched tools and other lithic artefacts: (A) Frontal scraper with lateral side-scraper and used edge (SPN-6); (B) Discoidal banded agathe (SPN-6) and unmodified quartz crystal (TU-68); (C) Frontal end-scraper (TUI-5); (D) ovoidal end-scraper; (E) micro-drills (TA-1 and TU-67); (F) Frontal end-scraper (SPN-19-20); (G) Lateral side-scraper (TA-1); (H) Frontal end-scraper (TA-1); (I) flat-flake with ultramarginal retouching (TU-68) (TA-1); (J) Rabot / facial core (TUI-5); (K) Mortar and handstone/pestle (TA-1).

Figure 12. Bifacial tools: (A) Non-stemmed, triangular “Tuina”; (B) Stemmed, barbed “Punta Negra”; (C) Stemmed with shoulders “Fishtail”; (D) Stemmed “San Martín”; (E) Biface; (F) Non-stemmed, triangular “Tambillo”; (G) Pentagonal.

### Tables titles

Table 1. Archaeological sites and <sup>14</sup>C dates

Table 2. Locational patterns and environmental settings

Table 3. Projectile point type by raw material

### Tables

Table 1

| Site     | <sup>14</sup> C yr BP | cal yr BP<br>(95.4%<br>probability) | Lab. code       | Dated<br>material   | Reference                 |
|----------|-----------------------|-------------------------------------|-----------------|---------------------|---------------------------|
| TUI-1    | 10820±630             | 14178-10753                         | SI-3112         | Charcoal            | Núñez et al.,<br>2005     |
|          | 9080±130              | 10520-9709                          | NR              | Charcoal            |                           |
| TUI-5    | 10060±70              | 11805-11254                         | Beta-107120     | Charcoal            |                           |
|          | 9840±110              | 11614-10776                         | Beta 107121     | Charcoal            |                           |
| Tam-2/4a | 9590±110              | 11190-10580                         |                 |                     |                           |
| TA-1     | 8590±130              | 10119-9144                          | Beta-25536      | Charcoal            |                           |
|          | 8870±70               | 10178-9631                          | Beta-63365      | Charcoal            |                           |
| TU-67    | 8190±120              | 9435-8663                           | Beta-25535      | Charcoal            |                           |
| TU-68    | 9290±100              | 10682-10231                         | Beta-25532      | Charcoal            |                           |
| TU-109   | 10590±150             | 12725-11995                         | Beta-142172     | Charcoal            |                           |
|          | 8870±50               | 10158-9692                          | Beta-188223     | Charcoal            |                           |
| SL-1     | 10280±120             | 12645-11716                         | HV-299          | Charcoal            |                           |
|          | 10400±13              | 12424-11405                         | N-3423          | Charcoal            |                           |
|          | 9960±125              | 11947-11107                         | N-3423          | Charcoal            |                           |
| TUY-1    | 8130±110              | 9395-8633                           | BeTA-<br>105691 | Charcoal            |                           |
|          | 8210±110              | 9444-8771                           | Beta-105692     | Charcoal            |                           |
| AC-1     | 8720±100              | 10134-9487                          | Beta-105696     | Charcoal            |                           |
| SM-4     | 8130±50               | 9071-8650                           | Beta-116573     | Charcoal            |                           |
| SPN-1    | 9450±50               | 10775-10443                         | Poz-3274        | Peaty<br>sediments  | Grosjean et<br>al., 2005  |
|          | 10460±50              | 12543-12035                         | B-8150          | Peaty<br>sediments  |                           |
|          | 9180±50               | 10485-10206                         | B-8151          | Peaty<br>sediments  |                           |
|          | 10350±60              | 12409-11830                         | B-8152          | Peaty<br>sediments  |                           |
|          | 10440±50              | 12430-12020                         | B-8153          | Vegetal             |                           |
|          | 9230±50               | 10497-10240                         | B-8154          | Peaty<br>sediments  |                           |
|          | 10470±50              | 12545-12050                         | B-8155          | Peaty<br>sediments  |                           |
| SPN-6    | 10260±60              | 12068-11652                         | Beta-191578     | Charcoal            | Cartajena et<br>al., 2014 |
|          | 10000±50              | 11693-11240                         | Beta-309834     | charred<br>material |                           |



|           |         |             |             |                  |  |
|-----------|---------|-------------|-------------|------------------|--|
| SI-7      | 9940±50 | 11601-11204 | Beta-309833 | organic sediment |  |
|           | 9950±50 | 11604-11220 | Beta-309831 | charred material |  |
| SPN-19/20 | 9460±50 | 11065-10513 | Beta-309833 | charred material |  |
|           | 9480±50 | 11070-10560 | Beta-309828 | Organic sediment |  |

Table 2

| Site      | Elevation (masl) | Vegetation belt | Settlement type | Geoform                            | Macro-geoform            | Litho-stratigraphic unit  |
|-----------|------------------|-----------------|-----------------|------------------------------------|--------------------------|---|
| TUI-1     | 3117             | Prepuna         | Rockshelter     | Hillside-ravine                    | Domeyko precordillera    | CP-2. Continental marine and volcanic sequences (Carboniferous-Permian)   |
| TUI-5     | 3174             | Prepuna         | Cave            | Ravine bottom                      | Domeyko precordillera    | CP-2. Marine and continental volcanic sequences (Carboniferous-Permian)<br>Qa. Alluvial deposits, subordinately colluvial |
| Tam-1     | 2348             | Desert          | Open site       | Phreatic beach                     | Atacama basin depression | Qa. Alluvial deposits, subordinately colluvial or lacustrine (Pleistocene-Holocene)                                       |
| TU-67     | 2567             | Desert          | Cave            | Ravine wall                        | Western cordillera       | Qa. Alluvial deposits, subordinately colluvial or lacustrine (Pleistocene-Holocene)                                       |
| TU-68     | 2454             | Desert          | Rockshelter     | Ravine wall                        | Western cordillera       | Qa. Alluvial deposits, subordinately colluvial or lacustrine (Pleistocene-Holocene)                                       |
| TU-109    | 2962             | Prepuna         | Rockshelter     | Ravine wall                        | Western cordillera       | P3t. Ignimbrites (Pliocene)   |
| SL-1      | 3264             | Prepuna         | Cave            | Ravine wall                        | Western cordillera       | PP1c. Sedimentary deposits (Pliocene-Holocene)  |
| TUY-1     | 4070             | High-Puna       | Open site       | Lacustrine beach                   | Salars depression        | P3i. Volcanic centers (Pliocene)  |
| AC-1      | 4205             | High-Puna       | Open site       | Lacustrine terrace                 | Salars depression        | P3t. Ignimbrites (Pliocene)   |
| SM-4      | 3695             | High-Puna       | Open site       | Lacustrine terrace                 | Western cordillera       | PP1c. Sedimentary deposits (Pliocene-Holocene)  |
| SPN-1     | 2978             | Prepuna         | Open site       | Fluvial terrace and phreatic beach | Preandean basins         | Qe. Aeolian deposits (Pleistocene-Holocene)   |
| SPN-6     | 3018             | Prepuna         | Open site       | Phreatic beach                     | Preandean basins         | PP1c. Sedimentary deposits (Pliocene-Holocene)  |
| SI-7      | 3019             | Prepuna         | Open site       | Phreatic beach and fluvial terrace | Preandean basins         | Qa-alluvial deposits, subordinately colluvial or lacustrine (Pleistocene-Holocene)  |
| SPN-19/20 | 2960             | Prepuna         | Open site       | Playa freática                     | Preandean basins         | Qa-alluvial deposits, subordinately colluvial or lacustrine (Pleistocene-Holocene)  |

Table 3

| Projectile Point type   | Siliceous |        | Basalt |        | Obsidian |       | Tuff |        | Total |        |
|-------------------------|-----------|--------|--------|--------|----------|-------|------|--------|-------|--------|
|                         | n         | %      | n      | %      | n        | %     | n    | %      | n     | %      |
| Fishtail                |           | 0,00%  |        | 0,00%  | 1        | 2,56% |      | 0,00%  | 1     | 0,96%  |
| Pentagonal              |           | 0,00%  | 2      | 6,06%  | 1        | 2,56% | 1    | 14,29% | 4     | 3,85%  |
| Stemmed barbed          | 6         | 24,00% |        | 0,00%  |          | 0,00% |      | 0,00%  | 6     | 5,77%  |
| Tetragonal (San Martín) |           | 0,00%  | 20     | 60,61% | 1        | 2,56% | 1    | 14,29% | 22    | 21,15% |

|                                    |    |         |    |         |    |         |   |         |     |         |
|------------------------------------|----|---------|----|---------|----|---------|---|---------|-----|---------|
| Triangular, non-stemmed (Tambillo) | 5  | 20,00%  | 3  | 9,09%   | 7  | 17,95%  | 3 | 42,86%  | 18  | 17,31%  |
| Triangular, non-stemmed (Tuina)    | 14 | 56,00%  | 8  | 24,24%  | 29 | 74,36%  | 2 | 28,57%  | 53  | 50,96%  |
| Total                              | 25 | 100,00% | 33 | 100,00% | 39 | 100,00% | 7 | 100,00% | 104 | 100,00% |